

Institutionen för systemteknik  
Department of Electrical Engineering

Examensarbete

**Model-Based Control of  
Two-Stage Turbochargers for  
Heavy-Duty Diesel Engines**

Master's thesis  
performed in **Vehicular Systems**

**Svante Löthgren**

LiTH-ISY-EX-14/4766-SE

Linköping 2014



**Linköpings universitet**  
**TEKNISKA HÖGSKOLAN**



# Model-Based Control of Two-Stage Turbochargers for Heavy-Duty Diesel Engines

Master's thesis  
performed in **Vehicular Systems**  
**Dept. of Electrical Engineering**  
at **Linköping University**

**Svante Löthgren**

LiTH-ISY-EX-14/4766-SE

Handledare: **Ph.D. Andreas Thomasson**, ISY, Linköping University  
**Anders Larsson**, NEPP, Scania CV

Examinator: **Associate Professor Lars Eriksson**, ISY, Linköping University

Linköping 2014-06-27



<b>Presentationsdatum</b> _____ 2014-06-13 <b>Publiceringsdatum (elektronisk version)</b> _____ 2014-06-27	<b>Institution och avdelning</b> <b>Institutionen för systemteknik</b>  <b>Department of Electrical Engineering</b>	 <b>Linköpings universitet</b>
---	--	--

<b>Språk</b> _____ Svenska <input checked="" type="checkbox"/> Annat (ange nedan)  _____ Engelska  <b>Antal sidor</b> _____ 74	<b>Typ av publikation</b> _____ Licentiatavhandling <input checked="" type="checkbox"/> Examensarbete _____ C-uppsats _____ D-uppsats _____ Rapport _____ Annat (ange nedan) _____	<b>ISBN (licentiatavhandling)</b>  <b>ISRN</b> <b>LiTH-isy-ex--14/4766--SE</b> <b>Serietitel (licentiatavhandling)</b>  <b>Serienummer/ISSN (licentiatavhandling)</b>
--	---	--

<b>URL för elektronisk version</b> <a href="http://www.ep.liu.se">http://www.ep.liu.se</a>
---

<b>Publikationens titel</b> Model-Based Control of Two-Stage Turbochargers for Heavy-Duty Diesel Engines  <b>Författare</b> Svante Löthgren
---

<p><b>Sammanfattning</b></p> <p>Konceptet downsizing är bevisligen en mycket kapabel lösning för att höja en motors verkningsgrad. Nyckelkomponenten är turbosystemet som använder överskottsenergi i avgaserna för att komprimera in luft till cylindern. Det finns olika typer av turbosystem, i denna uppsats modelleras en seriell turbostruktur tillsammans med en komplett sexcylindrig motor. En modellbaserad regulator utvecklas för att reglera insugstrycket. Regulatorn arbetar i moder som definieras av motorns arbetspunkt. För att styra turboladdningen på ett bra sätt är det viktigt att ha vetskap om energin i motorns avgaser, varpå mer dynamik har införts i befintlig temperaturmodell. Temperaturmätningar har lett till förvånande och teoretiskt motstridiga resultat. Detta har undersökts och förslag på förbättringar tas fram.</p> <p>Motormodellen har validerats och systemet tillsammans med regulatorn har utvärderats i simuleringsexperiment. Det seriella turbosystemet jämförs med ett VGT-system, varpå potentiella fördelar hos en seriell dubbelturbo diskuteras</p> <p><b>Abstract</b></p> <p>The concept of downsizing has proved to be a succesful method to improve engine efficiency. The engine key component is the turbocharging system that use excess energy in the exhaust gases to compress air into the cylinder. There are different types of supercharging systems, in the thesis a serial turbo system is modeled together with a complete six cylinder engine. A model-based controller is developed that regulates the intake pressure to a certain reference. The controller operates in modes that are defined by the engine operating point. To control the turbochargers it is necessary to have knowledge about the energy in the exhaust gases. A dynamic temperature model has therefore been analyzed, which has led to surprising results regarding the temperature measurements made in the test cells. This is analyzed and improvements are suggested. The engine model is validated and the system, including controller, is evaluated in certain simulations. The serial turbo concept is compared to a VGT turbo system, which gives a hint of the possible advantages of serial turbo charging.</p>
--

<b>Nyckelord</b> Turbo, Control, Model Based, Exhaust, MVEM
--



# Abstract

The concept of downsizing has proved to be a successful method to improve engine efficiency. The engine key component is the turbocharging system that use excess energy in the exhaust gases to compress air into the cylinder. There are different types of supercharging systems, in the thesis a serial turbo system is modeled together with a complete six cylinder engine. A model-based controller is developed that regulates the intake pressure to a certain reference. The controller operates in modes that are defined by the engine operating point. To control the turbochargers it is necessary to have knowledge about the energy in the exhaust gases. A dynamic temperature model has therefore been analyzed, which has led to surprising results regarding the temperature measurements made in the test cells. This is analyzed and improvements are suggested.

The engine model is validated and the system, including controller, is evaluated in certain simulations. The serial turbo concept is compared to a VGT turbo system, which gives a hint of the possible advantages of serial turbo charging.

# Sammanfattning

Konceptet downsizing är bevisligen en mycket kapabel lösning för att höja en motors verkningsgrad. Nyckelkomponenten är turbosystemet som använder överskottsenergi i avgaserna för att komprimera in luft till cylindern. Det finns olika typer av turbosystem, i denna uppsats modelleras en seriell turbostruktur tillsammans med en komplett sexcylindrig motor. En modellbaserad regulator utvecklas för att reglera insugstrycket. Regulatorn arbetar i moder som definieras av motorns arbetspunkt. För att styra turboladdningen på ett bra sätt är det viktigt att ha vetskap om energin i motorns avgaser, varpå mer dynamik har införts i befintlig temperaturmodell. Temperaturmätningar har lett till förvånande och teoretiskt motstridiga resultat. Detta har undersökts och förslag på förbättringar tas fram.

Motormodellen har validerats och systemet tillsammans med regulatorn har utvärderats i simuleringsexperiment. Det seriella turbosystemet jämförs med ett VGT-system, varpå potentiella fördelar hos en seriell dubbelturbo diskuteras.



# Acknowledgments

I would like to thank my examiner Lars Eriksson at Vehicular Systems and Henrik Flemmer at Scania CV for giving me the opportunity to write this thesis. It has been truly interesting and a lot of fun working with this task. Anders Larsson at Scania CV is acknowledged for interesting discussions and support. I would like to send a special thanks to my supervisor Andreas Thomasson, who is always guiding me in the right direction and helping me focus on the right problem areas. I also thank Oskar Leufvén for all the support and interesting discussions, Erik Höckerdal for helping me with my measurements and my master thesis colleagues at the office for the friendly and supportive environment. Thank you all for your time.

Finally, i would like to thank my family and friends for their care and support, especially my beloved Anna who is always supporting me in the right way.

*Svante Löthgren*



# Contents

<b>Contents</b>	<b>xi</b>
<b>Chapter 1</b>	<b>1</b>
1 <b>Introduction</b>	1
1.1 Background	1
1.2 Purpose and goal	2
1.3 Problem description	2
1.4 Overall approach	3
1.5 Expected results	3
<b>Chapter 2</b>	<b>5</b>
2 <b>Related work &amp; State of the Art</b>	5
2.1 Modeling	5
2.2 Control	6
<b>Chapter 3</b>	<b>7</b>
3 <b>System description</b>	7
3.1 Model	7
3.2 Control	8
<b>Chapter 4</b>	<b>9</b>
4 <b>Engine Model</b>	9
4.1 Engine modelling	9
4.2 Turbo model	9
4.2.1 Turbo maps	9
4.2.2 Implementing a turbomap	12
4.2.3 Compressor model	12
4.2.4 Turbine model	14
4.2.5 Turbo dynamics	15
4.2.6 Bypass and Wastegate actuators	16
4.2.7 Turbo scaling	17
4.3 Parametrization	18
4.3.1 Cylinder and throttle	18
4.3.2 Incompressible flow restriction	18
4.3.3 Intercooler temperature model	20
4.3.4 Wastegate and bypass valve validation	21
4.3.5 Validation compressor model	22

4.3.6	Validation turbine model . . . . .	23
<b>Chapter 5</b>		<b>25</b>
5	<b>Temperature model . . . . .</b>	<b>25</b>
5.1	Derivation of dynamic equations . . . . .	25
5.1.1	Gas temperature . . . . .	26
5.1.2	Wall temperature . . . . .	27
5.1.3	State space model . . . . .	28
5.2	Temperature measurements . . . . .	29
5.2.1	Experimental setup . . . . .	29
5.2.2	Experimental results . . . . .	30
5.2.3	Temperature measurements . . . . .	30
5.2.4	Suggested solution . . . . .	33
<b>Chapter 6</b>		<b>35</b>
6	<b>Controller design . . . . .</b>	<b>35</b>
6.1	Control problem . . . . .	35
6.2	Control approach . . . . .	36
6.2.1	Operating modes . . . . .	36
6.2.2	Mapping of modes . . . . .	36
6.2.3	Mode 0 . . . . .	38
6.2.4	Mode 1 and 3 . . . . .	39
6.2.5	Mode 2 . . . . .	39
6.3	Safety application . . . . .	40
6.3.1	Conditions and assumptions . . . . .	40
6.3.2	Observer design . . . . .	41
6.3.3	Limitation of control signal . . . . .	41
<b>Chapter 7</b>		<b>43</b>
7	<b>Results . . . . .</b>	<b>43</b>
7.1	Validation of model . . . . .	43
7.2	Validation of controller . . . . .	45
7.2.1	Throttle controller . . . . .	45
7.2.2	Serial turbo controller . . . . .	46
7.2.3	Turbo speed observer . . . . .	48
7.3	Simulation experiment . . . . .	50
<b>Chapter 8</b>		<b>55</b>
8	<b>Conclusions and future work . . . . .</b>	<b>55</b>
8.1	Conclusions . . . . .	55
8.2	Future work . . . . .	56
8.2.1	Engine model . . . . .	56
8.2.2	Controller . . . . .	56
8.2.3	Temperature measurement . . . . .	56
8.2.4	Temperature model . . . . .	56
<b>Bibliography</b>		<b>59</b>

Appendix A	61
Appendix B	73



# Chapter 1

## Introduction

In this chapter the introduction to the thesis work is given. The background to the problem is discussed and the purpose of solving it. This leads to a more specific description of the problem and a shorter explanation of the planned approach and expected results.

### 1.1 Background

The vehicle industry has to live up to requirements both from governments and the customers, and the demands are getting tougher and tougher to handle. Emission- and performance requirements forces the technological development of both software and hardware to be at the absolute forefront. A promising way to keep emission levels low but to still maintain high performance is to combine turbocharging techniques with recirculation of exhaust gases [1].

Turbocharging is a central part of the concept downsizing, where a smaller engine is turbocharged to have the ability to give high power when needed, but to keep the fuel consumption low in more normal operating points. This is achieved with the help of a turbocharger consisting of a compressor and a turbine connected with a shaft. In heavy-duty vehicles it is common to connect the compressor to a turbine with variable geometry (VGT). This type of turbo is preferred to fix-geometry turbochargers with wastegate because they can compress more air fast in a wider range of operating points [2]. However, the control and actuation of a VGT is more robust in the complicated environment (high temperature, high pressure and a gasmixture containing particles from the combustion process).

The maximum air velocity at the tip of the compressors rotorblade limits the maximum pressure ratio that can be delivered by the turbocharger. This means that the engines intake pressure is limited to a maximum level. By connecting more turbochargers in series, the pressure can be raised in steps and higher intake pressure gets possible. Since intake pressure is closely related to airflow, it means that it gets possible to inject more air into the combustion chamber [3], [4]. Considering the possibility to have different size on the turbochargers, the operating range can be improved since a smaller turbocharger is more efficient for low massflow and can spool up faster than a larger turbo [5]. The serial turbo is preferably designed with fix-geometry turbochargers with wastegate to achieve a robust system.

## 1.2 Purpose and goal

The purpose of the thesis is to analyze potential positive effects of a serial turbo with fix-geometry turbines with wastegate. This is done with a dynamic mean value engine model. One subtask will be to process the existing models describing the temperature in the exhaust manifold.

Based on the model, a controller should be designed. The controller will be helpful to show the potential positive effects of a serial turbo compared to existing engine system. The existing engine system could be the engine model created by J. Wahlström, which would be the reference model. It is also desirable to be able to connect the model to the driveline model created in [6]. Main objectives in the thesis:

1. Create a dynamic mean value engine model of a diesel engine with a serial turbo with wastegate. This is done by combining models from [1] and [7].
2. Process the existing exhaust gas temperature models. The focus in this task is not to analyze the chemical processes in the combustion chamber, but more on how the temperature varies in the exhaust manifold post-injection.
3. Take knowledge from 1 and 2 above to propose a controller that shows the potential positive effects of the serial turbo engine setup compared to existing system.

## 1.3 Problem description

In [1] a diesel engine with VGT and EGR is described together with some controlling tactics. It is explained that the dynamics in the engine creates a very complex controlling problem with non-minimum phase behaviour and sign reversal. In the thesis, the aim is also to analyze and describe the behaviour of a system, but for a serial turbo.

First, a model of a serial turbo has to be developed. The model in the thesis should be modular to conveniently be able to switch engine components if needed. This may simplify future work if other components behaviour and interaction is to be analyzed.

When knowledge of the system and its properties is gained, a controller should be designed. Several approaches are known, for example the performance can be improved by using the intake pressure as reference, or the pumping losses can be reduced by minimizing the exhaust pressure. According to [3] it is very complicated to combine all positive effects a serial turbo may have, it often gets to a trade-off between different properties that is balanced by the designer.

Since the controller will be model based, the model must describe the reality very well to achieve high controller performance. Temperature and pressure in the exhaust manifold is especially important for controlling the turbo (and EGR) setup, since the exhaust gas temperature is strongly connected to how much energy the turbocharger will receive [8].

## 1.4 Overall approach

The starting point of the thesis is a mean value engine model created by J. Wahlström [1] and a mean value engine model library created by L. Eriksson [7]. These two sources are combined to create a mean value model of a serial turbo. The model will be prepared for modeling EGR, but the thesis will not treat EGR further than that.

In the thesis a prototype of the model can not be provided, which means some complications with the validation of the model. In [1] a model is created, describing the same engine as the thesis is supposed to model. The only difference is the turbocharging of the engine, which in the thesis is done with a serial turbo, and in J. Wahlströms model is done with a VGT. Since the engine part of the model should be identical, [1] can be used as a reference. This means that in the end of the thesis, conclusions about the differences can be made.

## 1.5 Expected results

The thesis is expected to end up in a complete validated six-cylinder engine model with a serial turbo. The model will be calibrated to match measured data. However, when comparing the serial turbo and the VGT model, small differences are expected. This is due to an additional intercooler temperature model in the serial turbo, and also a small difference in the control volume model structure.

The intake pressure will be controlled by a suggested controller, that follows a given reference. The controller will follow the given reference without extreme overshoots, oscillations or bumps in mode switches. The turbo charging system will operate under safe conditions since a turbo speed observer will be implemented, that estimates the turbo speed with desired precision. This estimation is used by the controller to limit the control signals.



# Chapter 2

## Related work & State of the Art

In this chapter the state of the art in the current field is presented. A walkthrough is done to clarify what has already been done and what are the complications. The purpose of this is to give the reader input on possibilities and difficulties within this field of research. Since the approach in the thesis is model-based control, this literature study is divided in two sections; modeling and control.

### 2.1 Modeling

The foundation of the modeling done in the thesis is made of the model library made by L. Eriksson [7] together with a model made by J. Wahlström [1]. The last mentioned model describes a diesel engine with VGT and EGR. Erikssons library is modularised to conveniently have the opportunity to evaluate and analyze different engine configurations. Wahlströms model is modified and some components are replaced with components from Erikssons library to receive an engine with serial turbo.

As for engines with serial turbo it considered in [3, 9] to be a very capable solution to the problem described in section 1.3. Despite the introduction of one more restriction in the form of one more turbocharger, the engines total ability to transform energy increases, and the delivered power from the engine may increase [3]. In [9] different types of serial turbos are compared and what properties they bring to the engine. It is an interesting paper where two serial fix-geometry turbos with wastegate appear as a robust and straightforward method, while other configurations often creates more complicated systems.

Since the focus in the thesis is turbocharging and its control, an accurate description of the exhaust gas temperature is very important [8, 10]. This is because the exhaust gas temperature is strongly coupled to how much energy that is entering the turbine. When the exhaust gas leaves the combustion chamber, the temperature and pressure is relatively high. This makes it a bad environment for sensors. In [8] a pressure estimator is developed based on the states after the two turbines. This is normally a better environment for sensors which could lead to a more robust system.

The development of temperature models seems to have slowed down. In [10] most work up to that time is summarized. After that article it is noticed that most research is done from a CFD-perspective. That does not fit the purpose of the thesis since the goal is to create a fast and simple model that describes interesting states accurately. The CFD-approach seems to be demanding to much computational power, but maybe it is the right approach for future model development.

## 2.2 Control

Wahlström is describing the interaction between VGT and EGR in detail in [1]. The two gas-loops creates a complex non-linear control problem with sign reversal. Several similar studies have been done with different control algorithms applied. Not that many studies seems to have been made on serial turbo systems which means that the knowledge of such system and its control problem not yet is as well defined as other systems [11]. There are different control strategies depending on the priorities of the designer. If performance is a priority, it is common to have a relatively high pressure in the intake manifold which means a fast torque response and a faster system. If lower fuel consumption and emissions is a priority, the pumping losses should be minimized, which is done in [1]. In [4] the control algorithm is based on a model where the high pressure turbo (the turbo close to the engine) is of VGT type. The control strategy is a LQG-controller that is linearized in different working points. This type of linearization is common according to [12]. In [13] a feedback with IMC-structure with a non-linear feedforward is implemented to control a model consisting of a two fix-geometry turbos with wastegate actuation. In this complex controller no linearization is made which affects the results positively but the robustness negatively.

A more straightforward solution is presented in both [14] and [11], where the approach is based on cascade control. This seems like a suitable approach since several measured signals can be used in the controller. The cascade controllers performance is also improved if the inner loop is faster than the outer [15]. In this case, the inner loop is made out of the high pressure turbo which is smaller than the low pressure turbo which would be the outer loop. In [11] there is an interesting discussion about whether the pressure sensor in the exhaust manifold is necessary or not. In the thesis the necessary signals is assumed to be available, which seems like a good approach in a first stage. But the question of how many (if any) extra sensors is needed in the serial turbo structure is vital for future work. It is noticed that in most publications the step responses for different subsystems is analyzed in an early stage. This often makes the foundation for the controller [1, 11, 14].

The most common control approach in studied literature is to divide the engines operational points in three different modes; one where only the high pressure turbo is activated, one where only the low pressure turbo is activated and one mode where they work together (and of course one more mode where no charging is needed). In the different modes the serial turbo is then controlled to deliver a certain demanded intake pressure [14]. There are strong coupling between intake pressure and the turbos angular velocity, but no studies have been found where the control has been made with respect to this.

# Chapter 3

## System description

The following chapter briefly describes the system that is to be analyzed and controlled. The purpose of this is to give the reader an overview which might give an understanding for the bigger picture and the most important components. A more detailed description of the engine is given in chapter 4.

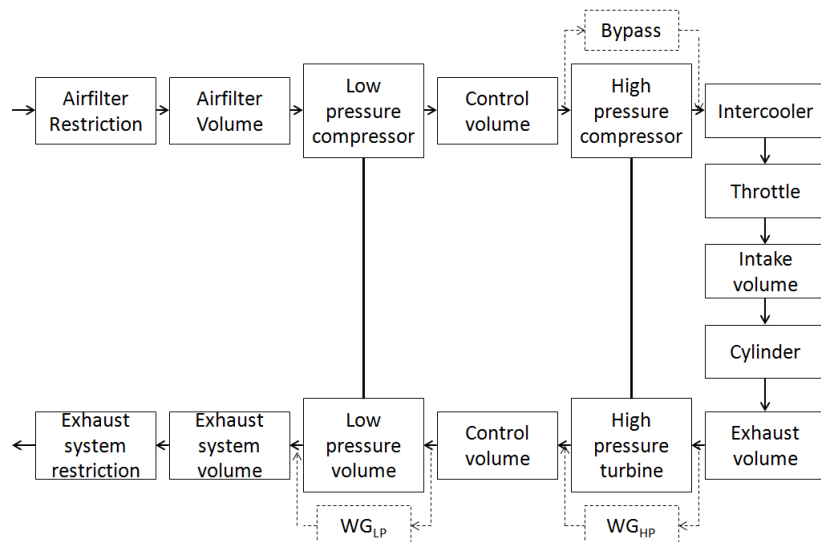


**Figure 3.1:** Model structure of an engine with a serial turbo. The arrows shows the airflow through the components.

### 3.1 Model

In figure 3.1 above the engine model is described as a block diagram, where the arrows represent the airflow through the components. Every block contains a set of equations that describes the components dynamic behaviour. The base structure for this model is made of [1, 7]. The models are implemented with embedded Matlab in Simulink to conveniently be able to automatically generate C-code from the model. The purpose of representing the model as C-code is to facilitate future work and implementation in for example some kind of HIL-testing.

The focus in the thesis will be at the turbochargers, and mostly on the hot side i.e post injection. It is a complex part of the engine to model since the flowcharacter is hard to

predict and the temperatures are relatively high [16]. Although the model is very important to be able to control the turbocharging in a good way.

To reduce turbo-lag and improve the operating range, the turbochargers will be scaled. The larger turbo will be scaled to 60 % of its size, and is implemented closest to the engine. This will be utilized by the controller.

Another important question is if any extra sensors has to be added to the engine compared to a regular single turbo. In the thesis it will be assumed that the temperature and pressure between the compressors is measured, the question about additional sensors contra observability is left for future work.

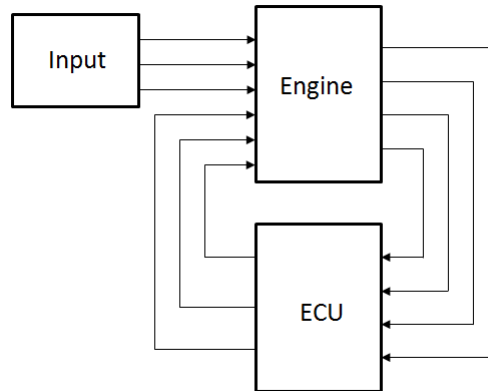


**Figure 3.2:** *The input is the reference which is set by the driver. The controller is implemented in the ECU.*

### 3.2 Control

The environment is described in figure 3.2 above, where the controller is implemented in the ECU-block. The ECU will receive a set of measured signals as input and generate control signals to the actuators as output.

One important principle the controller will use is that the turbo closest to the engine, named high pressure turbo, is smaller than the other turbo. A smaller turbo has less inertia which means that the high pressure turbo will accelerate faster than the low pressure turbo. This is used to reduce turbo-lag and improve the operating range. However, a smaller turbo has a tendency to overspeed at high massflow, which is why a safety function is implemented. An observer supervise the turbochargers speed and a limiter that limits the control signal is implemented. The controller operates in three modes that are chosen based on the engine operating point, which is coupled to the compressor efficiency. This is explained further in chapter 6.

# Chapter 4

## Engine Model

Since the thesis mainly focus on turbocharging, this chapter only shows the mathematical equations that describes the turbochargers. The complete engine model is stated in appendix A.

### 4.1 Engine modelling

The engine that is modelled is a six-cylinder heavy-duty engine with two turbochargers in series that are actuated by wastegate. Inspiration to the model is mainly received from [1, 17, 18, 19, 20]. Since no serial turbo can be provided for measurements, the model described in [1] will be used for validation. All models are implemented componentwise to facilitate future work and the analyze of different engine setups. All equations and signal definitions of the engine components are stated and described in appendix A.

### 4.2 Turbo model

In the following section the turbo model is explained, both compressor, turbine and its dynamics. Also, a short description of a turbo map is made.

#### 4.2.1 Turbo maps

Turbo maps are used to describe a turbochargers performance in different operating points. This is the key to describing the turbo, in other words it is the reference. It is a complicated process to create a turbo map and one should always remember that the mapping is made by man and different factors can affect whether to trust the map or not. A deeper study of turbo maps is made in [19].

Corrected variables are used in the turbo map in order to make it valid for all circumstances, not only for the environment where the map was made. The inlet conditions may of course vary, but also the ambient conditions may differ a lot depending on where the engine is running. One example of this is a truck driving from sea-level through a mountain pass, where the ambient pressure will change. As a compensation for this, corrected variables are used in the design process. Below is a short description of what a standard turbomap contains [21]. It is divided into one compressor part and one turbine part.

### Compressor map

In the compressor part of the turbomap there are four interesting variables; massflow, pressure ratio, speed and efficiency. These variables are enough to get a good picture of the performance of the compressor. Notice that the massflow and speed are corrected variables and that efficiency means the adiabatic efficiency. The *corrected massflow* is explained below.

$$\dot{m}_{c,corr} = \dot{m}_c \frac{\sqrt{\frac{T_{01}}{T_{c,ref}}}}{\frac{p_{01}}{p_{c,ref}}} \quad (4.1)$$

Where  $\dot{m}_c$  is the true, non-scaled massflow through the compressor,  $T_{01}$  is the inlet temperature,  $p_{01}$  is the inlet pressure,  $T_{c,ref}$  and  $p_{c,ref}$  are the reference values for temperature and pressure respectively. The compressor *pressure ratio* is described by the following equation.

$$\Pi_c = \frac{p_{02}}{p_{01}} \quad (4.2)$$

Where  $p_{02}$  is the outlet pressure, which means that when the compressor is activated the pressure ratio is larger than one. The *corrected compressor speed* is defined as follows.

$$N_{corr} = N_{tc} \frac{1}{\sqrt{\frac{T_{01}}{T_{c,ref}}}} \quad (4.3)$$

In above, the  $N_{tc}$  is the real, non-scaled turbo speed. The *adiabatic efficiency* is described below.

$$\eta_c = \frac{\Pi_c^{\frac{\gamma_c-1}{\gamma_c}} - 1}{\frac{T_{02}}{T_{01}} - 1} \quad (4.4)$$

Where  $\gamma_c$  is the ratio of specific heat. The equation describes how efficient the compression process is compared to an adiabatic process, i.e how the pressure increases in relation to how the temperature increases. In an ideal adiabatic process there is no heat transfer to the surroundings.

When measuring the compressor map, the compressor speed is fixed and the massflow and pressure ratio is varied. This is done for several speeds. The result is so called speed lines, who will have an upper limit where surge occur, and a lower limit where the compressor chokes.

### Turbine map

The turbine map also contains four interesting variables; massflow, expansion ratio, speed and efficiency. Massflow and speed are corrected values and the efficiency is the adiabatic efficiency. The turbine map usually also contains a flow parameter TFP and its reduced speed TSP.

The *corrected massflow* is given by the following equation.

$$\dot{m}_{t,corr} = \dot{m}_t \frac{\sqrt{\frac{T_{03}}{T_{t,ref}}}}{\frac{p_{03}}{p_{t,ref}}} \quad (4.5)$$

Where  $T_{t,ref}$  and  $p_{t,ref}$  are the reference temperature and pressure respectively.  $\dot{m}_t$  is the massflow passing through the turbine,  $T_{03}$  and  $T_{04}$  is the temperature at the inlet and outlet respectively.  $p_{03}$  is the inlet pressure and  $p_{04}$  is the outlet pressure. The massflow through the turbine is often represented by the *turbine flow parameter*,  $TFP$ , which is described below.

$$TFP = \dot{m}_t \frac{\sqrt{T_{03}}}{p_{03}} \quad (4.6)$$

The turbines *expansion ratio* is shown below.

$$\Pi_t = \frac{p_{03}}{p_{04}} \quad (4.7)$$

This variable is often inverted, it may vary. This means that the designer has to pay extra attention to this variable. The *corrected speed* follows the scaling shown in the equation below.

$$N_{t,corr} = N_{tc} \frac{1}{\sqrt{\frac{T_{03}}{T_{t,ref}}}} \quad (4.8)$$

As for the corrected massflow, the speed is often represented by another variable, namely the reduced speed expressed as the *turbine speed parameter*,  $TSP$ .

$$TSP = N_{tc} \frac{1}{\sqrt{T_{03}}} \quad (4.9)$$

As shown above the reference values is removed when expressing  $TFP$  and  $TSP$ . This means that the turbine speed only is scaled with the factors shown in the equations above. The *adiabatic efficiency* is shown below.

$$\eta_t = \frac{1 - \frac{T_{03}}{T_{04}}}{1 - \left(\frac{p_{04}}{p_{03}}\right)^{\frac{\gamma_t - 1}{\gamma_t}}} \quad (4.10)$$

Where  $\gamma_t$  is the ratio of specific heat for the exhaust gases passing through the turbine. The exhaust gas temperature is often relatively high, which can complicate measurements. Because of this, another equation is available that is based on the compressor power as shown below.

$$P_c = \dot{m}_c c_{p,c} (T_{02} - T_{01}) \quad (4.11)$$

Where  $c_{p,c}$  is the specific heat at constant pressure at the compressor. This equation can be used to express the efficiency according to the equation below.

$$\tilde{\eta}_t = \eta_t \eta_m = \frac{\dot{m}_c c_{p,c} (T_{02} - T_{01})}{\dot{m}_t c_{p,t} T_{03} \left(1 - \left(\frac{1}{\Pi_t}\right)^{\frac{\gamma_t - 1}{\gamma_t}}\right)} \quad (4.12)$$

Where  $\eta_m$  is the mechanical efficiency of the turbo shaft. For further reading about turbo maps, [19] is highly recommended.

### 4.2.2 Implementing a turbomap

The turbo map describes the properties of the turbocharger and there are mainly two ways of implementing it - either describing the map with mathematical equations or implement the whole map as a look-up table and extrapolate the demanded data. In the thesis a mathematical model is used.

A mathematical model can easily be manipulated to match mapped data very well in a desired operating range, but there are few models that match data over the whole operating range. For example one can compare one of the more simpler models described in [17] with a more advanced model described in [19]. It is clear that the more advanced model matches the data in what is seen as the whole operating range. But the simpler model match data well in some parts of the operating range, and this part is easy to move around and manipulate. It all depends on in what way the designer intend to use the model. In the next section the models are shown.

### 4.2.3 Compressor model

The two compressors will be modelled in the same way, the difference will be in the physical properties (size) and the estimated parameters who are depending on the maps. Since the two turbos will have different size, their behaviour will differ i.e the maps will differ. See section 4.2.7

#### *Input*

Variable	Unit	Description
$\omega_{tc}$	rad/s	Turbo speed
$p_{us}$	Pa	Upstream pressure
$p_{ds}$	Pa	Downstream pressure
$T_{us}$	K	Upstream temperature

#### *Output*

Variable	Unit	Description
$Tq_c$	Nm	Torque demanded by compressor
$\dot{m}$	kg/s	Massflow through compressor
$T_c$	K	Temperature of the massflow

#### *Parameters*

Variable	Unit	Description
$D_c$	m	Compressor diameter
$\Pi_{c,max}$	-	Maximum pressure ratio
$\Psi_{max}$	-	Maximum energy transfer coefficient
$c_p$	J/kgK	Specific heat capacity
$\gamma$	-	Ratio of specific heat
$\eta_{c,max}$	kg/s	Maximum efficiency
$\dot{m}_{c,corr,max}$	kg/s	Maximum corrected massflow
$Q_{11}, Q_{12}, Q_{22}$	-	Constants in efficiency model
$p_{ref,c}$	Pa	Reference pressure
$T_{ref,c}$	K	Reference temperature

## Equations

$$U_2 = \frac{D_c \omega_c}{2} \quad (4.13)$$

$$\Psi = 2c_p T_{us} \frac{\left(\Pi^{\frac{\gamma-1}{1}} - 1\right)}{U_2^2} \quad (4.14)$$

$$\Phi = \sqrt{\frac{1 - \Psi^2 K_1}{K_2}} \quad (4.15)$$

$$\dot{m}_c = \Phi \frac{U_2 p_{us} \pi D^2}{T_{us} 4R} \quad (4.16)$$

$$\eta_c = \eta_{c,max} - \chi^\top Q_\eta \chi \quad (4.17)$$

$$\chi = \begin{bmatrix} \Phi - \Phi_{max} \\ N_{c,corr} - N_{c,corr,max} \end{bmatrix} \quad (4.18)$$

$$Q_\eta = \begin{bmatrix} Q_{11} & Q_{12} \\ Q_{12} & Q_{22} \end{bmatrix} \quad (4.19)$$

$$T_c = T_{us} \left( \frac{\Pi_c^{\frac{\gamma-1}{\gamma}} - 1}{\eta_c} + 1 \right) \quad (4.20)$$

$$T_{qc} = \frac{P_c}{\omega_c} = \frac{\dot{m}_c c_p (T_c - T_{us})}{\omega_c} \quad (4.21)$$

The parameters are estimated using the compressormap based on stationary measurements. The estimation is done with curvefitting.

#### 4.2.4 Turbine model

The massflow through the turbine is described by a model that has no physical relation, but that has shown to give a good match to data [18]. The efficiency is modelled as a parabolic function of the blade speed ratio, BSR.

##### Input

Variable	Unit	Description
$p_{us}$	Pa	Upstream pressure
$p_{ds}$	Pa	Downstream pressure
$T_{us}$	K	Upstream temperature
$\omega_{tc}$	rad/s	Turbo speed
$A_{wg}$	m <sup>2</sup>	Effective flowthrough area, wastegate

##### Output

Variable	Unit	Description
$T_{ds}$	K	Downstream temperature
$\dot{m}_{ds}$	kg/s	Downstream massflow
$Tq_t$	Nm	Torque from turbine

##### Parameters

Variable	Unit	Description
$c_p$	J/kgK	Specific heat capacity
$\gamma$	-	Ratio of specific heat
$C$	-	Scaling factor turbine capacity
$K$	-	Fitting parameter choke function
$r_t$	m	Turbine blade radius
$\eta_{t,max}$	-	Maximum efficiency
$BSR_{opt}$	-	Blade speed ratio at maximum efficiency

##### Equations

$$Tq_t = \frac{\dot{m}_t c_p T_{em}}{\omega_{tc}} \left[ 1 - (\Pi_t)^{\frac{\gamma-1}{\gamma}} \right] \eta_t \quad (4.22)$$

$$MFP = C \sqrt{1 - \frac{1}{\Pi_t^K}} \quad (4.23)$$

$$\dot{m} = \frac{p_{em}}{\sqrt{T_{em}}} MFP \quad (4.24)$$

$$BSR = \frac{r_t \omega_{tc}}{\sqrt{2c_p T_{em} \left( 1 - \Pi_t^{\frac{1-\gamma}{\gamma}} \right)}} \quad (4.25)$$

$$\eta_t = \eta_{t,max} \left( 1 - \left( \frac{BSR - BSR_{opt}}{BSR_{opt}} \right)^2 \right) \quad (4.26)$$

The turbine actuator (wastegate) is modeled as a first order system with a time delay. The parameters in the model stated above is estimated with the turbine map, which is shown in section 4.3.6.

#### 4.2.5 Turbo dynamics

The shaft connecting the compressor and turbine is adding dynamics to the system due to inertia, friction and damping. Friction and damping is merged to one constant.

##### *Input*

Variable	Unit	Description
$T_{q_c}$	Nm	Torque demanded by the compressor
$T_{q_t}$	Nm	Torque from turbine

##### *Output*

Variable	Unit	Description
$\omega_{tc}$	rad/s	Turbo speed

##### *Parameters*

Variable	Unit	Description
$J_{tc}$	kg/m <sup>2</sup>	Inertia of the shaft
$d_{tc}$	kgm <sup>2</sup> rad/s	Friction- and dampingfactor

##### *Equations*

$$\frac{d}{dt}\omega_{tc} = \frac{1}{J_{tc}} (T_{q_t} - T_{q_c}) - d_{tc}\omega_{tc} \quad (4.27)$$

#### 4.2.6 Bypass and Wastegate actuators

The wastegate valves are the actuators for the turbocharger system together with the bypass valve. The massflow through the valves are modeled the same way as for the throttle, see appendix A. However, the actuator models differ. These valves are modeled as a first order system with a time constant.

##### *Input*

Variable	Unit	Description
$u_v$	—	Control signal to the valve

##### *Output*

Variable	Unit	Description
$A_{eff,v}$	$m^2$	Effective flowthrough area of the valve

##### *Parameters*

Variable	Unit	Description
$\tau_v$	$s$	Time constant of the valve

##### *Equations*

$$\dot{u}_v = \frac{1}{\tau_v} (u_v - \tilde{u}_v) \quad (4.28)$$

$\tau_v$  may be estimated by analyzing stepresponses in the control signal.

#### 4.2.7 Turbo scaling

One turbo map for a standard fix-geometry turbo is provided. This turbo is originally designed to operate alone in a truck, which is why this turbo will serve as low pressure stage. To get a suitable model for the high pressure turbo the given map is scaled.

The choice of turbo sizes is an important design task that affects the flexibility and efficiency of the whole engine. The matching is not a simple task since the smaller high pressure turbo has to be able to deliver desired massflow and pressure ratio at low speeds. For higher speeds the sharing of workload between the turbos and the phasing out of the high pressure stage is crucial for the engine efficiency. This is further discussed in [5].

In the thesis a simple scaling method will be used. The goal is to achieve a turbo about 60 % the size of the turbo given and use it as high pressure turbo. The calculations will go under certain assumptions, described in the following.

The first assumption is that the ability to compress air will not change with different turbo size, ie the pressure ratio in the turbo map will not be scaled. Because of the smaller turbo the massflow through the compressor is considered to be 60 % of that given for the low pressure turbo. The high pressure turbo speed should match the massflow which is why the turbine speed is increased accordingly. It is all straightforward - a smaller turbo is as capable of compressing air as a bigger turbo, but can do it for lower massflows. It will also rotate faster for a certain massflow than a larger turbo.

The efficiency of the scaled turbo is considered to be equal to the original turbo map.

The diameter of the high pressure turbo is considered to be 60 % of the low pressure turbo. This affects the turbo inertia quadratically since the inertia is proportional to the radius squared.

The two turbo maps are plotted in figure 4.1 below.

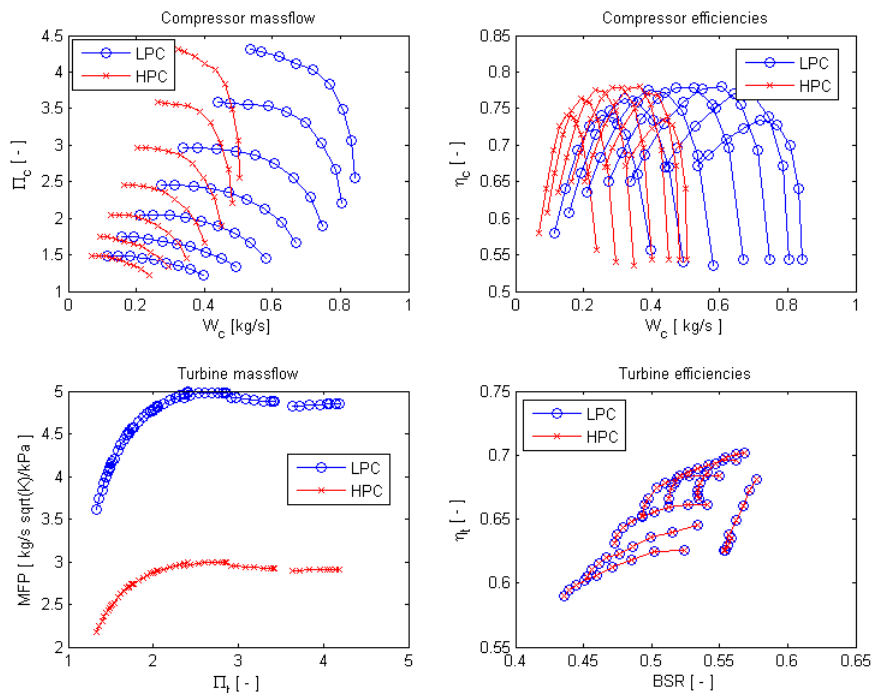


**Figure 4.1:** The provided low pressure turbo map is compared to the scaled high pressure turbo map.

### 4.3 Parametrization

In this section it is explained and shown how the model is parameterized to behave as the physical components it is supposed to describe.

#### 4.3.1 Cylinder and throttle

The parametrization of the cylinder and the throttle is taken straight from [1]. This gives a good reference for these parts of the engine setup, i.e the only thing that is modified in this work compared to mentioned reference is the gas exchange system. This makes the comparison easier.

The parametrization has been made in four steps. First, the static parameters are calculated for each subsystem with least square method. The same method is then used to optimize the static parameters for the whole model globally. In step three the actuators parameters are optimized to fit dynamic data. The last step is to optimize the other dynamic parameters for the whole model globally.

#### 4.3.2 Incompressible flow restriction

The three incompressible flow restrictions are the airfilter, the intercooler and the after treatment system. The flow restriction parameter  $H_r$  is calculated by least square curve-fitting. This requires knowledge of the massflow through the component, the upstream pressure and temperature and the downstream pressure in a stationary operating point. The more data points, the better the estimation. The results are presented in the following figures.

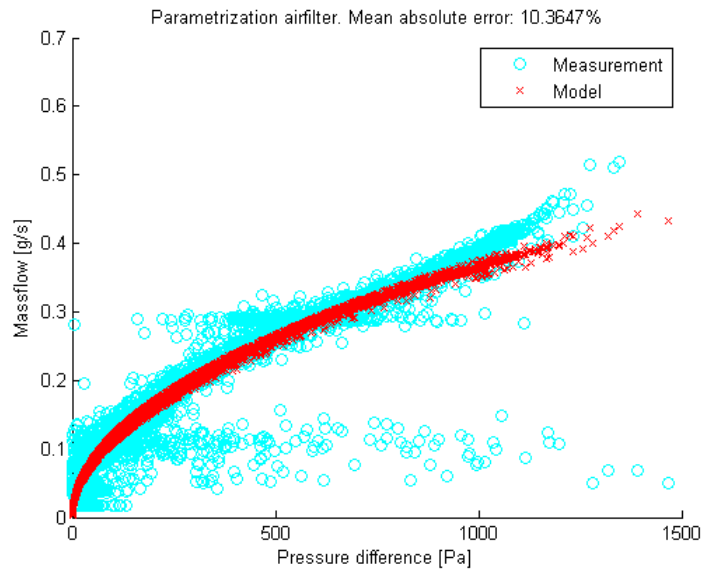


**Figure 4.2:** Validation of the air filter flow restriction. The estimation is made in 5000 stationary points. The model fits the measurements well, apart from some datapoints that stand out. No compensation has been made for them.

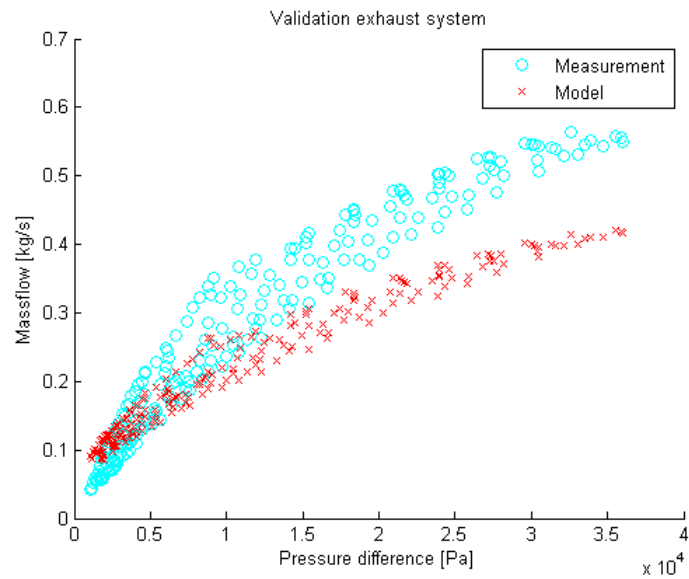


**Figure 4.3:** Validation of the exhaust system flow restriction. It is clear that the model gives a better fit for low pressure differences. For higher pressure difference the massflow will be modeled a bit too low.

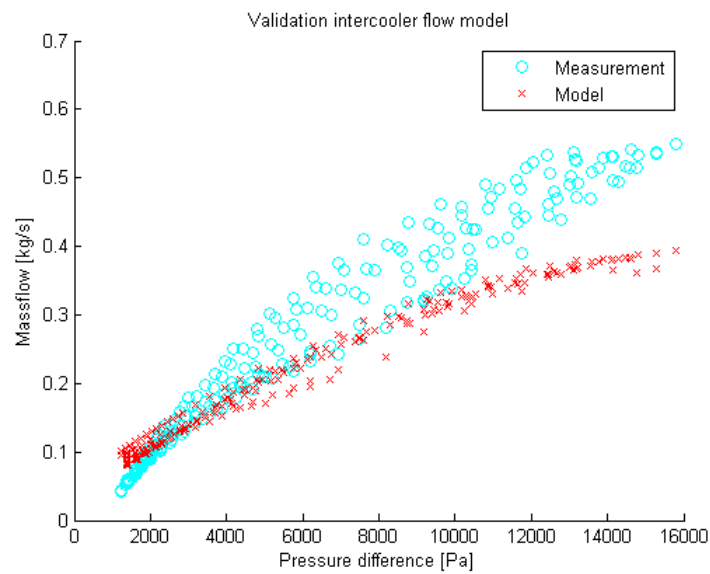


**Figure 4.4:** Validation of the intercooler flow restriction. The model gives good fit for low pressure difference, but estimates the massflow a bit too low for higher pressure differences.

It is noticed that the incompressible flow restriction model gives a better fit for low pressure difference compared to high.

### 4.3.3 Intercooler temperature model

The intercooler temperature is modeled by a simplified version of a regression model suggested in [17]. The coolants massflow is not considered in the thesis due to lack of measured data. The model is saturated to make sure that the temperature out of the intercooler is not lower than the coolant. The parameters are estimated with the method of least squares, and requires measurements of the up- and downstream temperature, the cooling temperature and the massflow through the intercooler in a stationary operating point. The model validation is illustrated in figure 4.5 below.

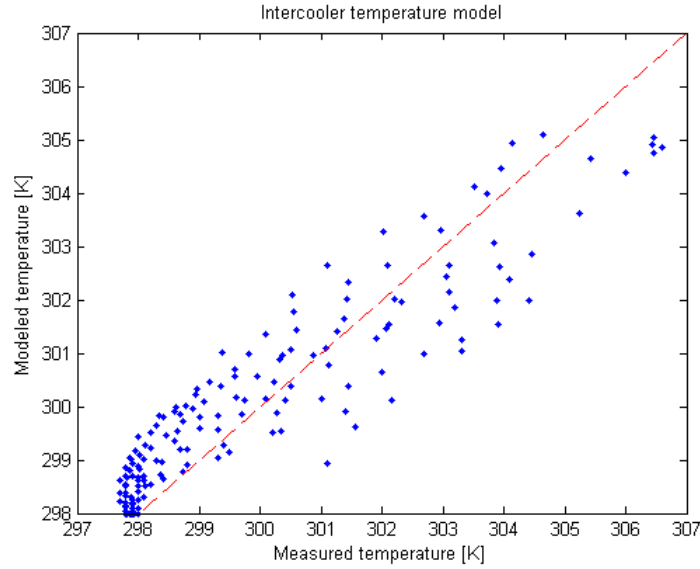


**Figure 4.5:** Validation of the intercooler temperature model. The model gives a good fit in a large part of the measured range, the absolute mean relative error is small.

The model works well in a large operating range. Since temperature differences are not that large, the relative error is small.

#### 4.3.4 Wastegate and bypass valve validation

The wastegates and the bypass valve are modeled as actuators with first order systems with a time constant. The bypass actuator is assumed to have same dynamics as the wastegates. The model can be rewritten as shown below.

$$\frac{d\tilde{u}_v}{dt} = \frac{1}{\tau} (u_v - \tilde{u}_v) \rightarrow \tilde{u}_v = u_v(1 - e^{-\frac{t}{\tau}}) \quad (4.29)$$

The above stated equation means that the time constant is equal to the time it takes for the step response to reach 63 % of the reference value. This is illustrated in figure 4.6 below.

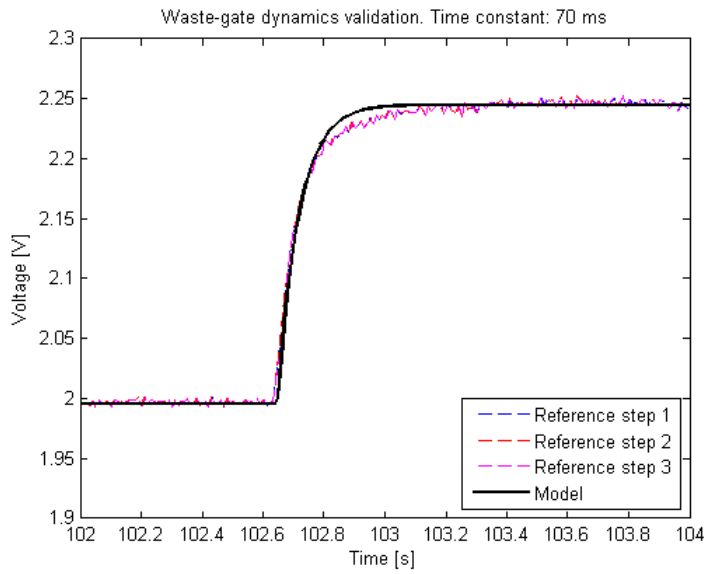


**Figure 4.6:** Validation of the time constant in the actuator valves. The time constant is calculated to 70 ms.

### 4.3.5 Validation compressor model

The compressor model described in section 4.2.3 is validated below, both for low- and highpressure turbo. There results are presented in figure 4.7.

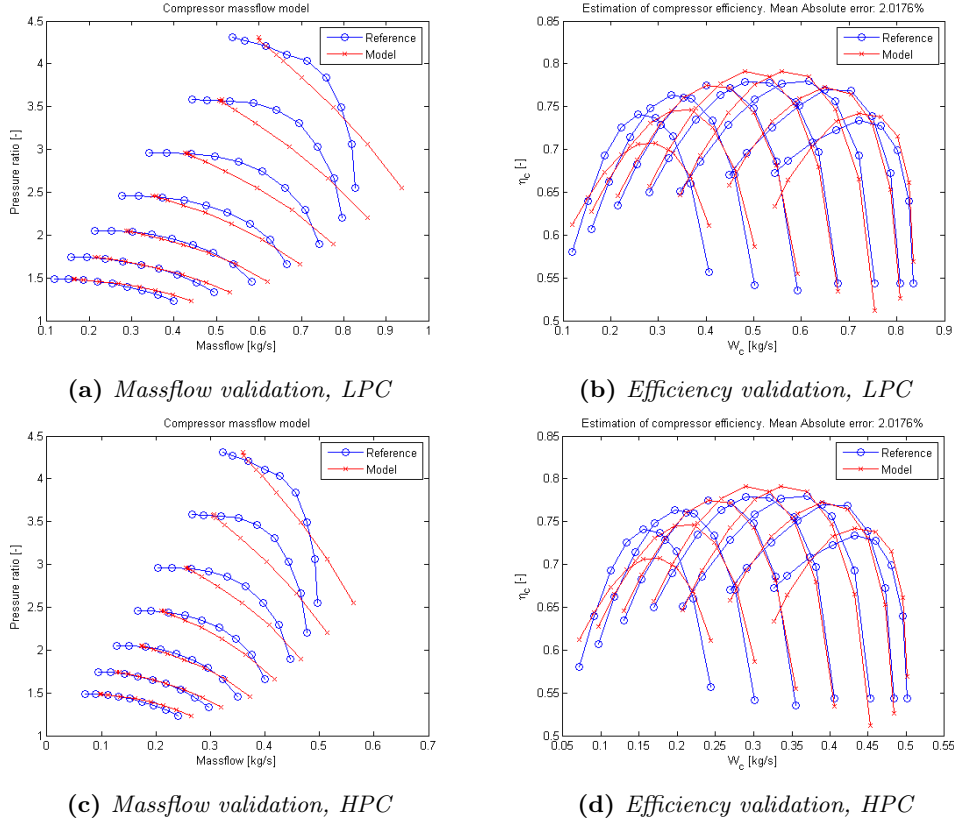


**Figure 4.7:** Validation of compressor model. First row is describing the low pressure compressor and the second row is describing the high pressure compressor.

The model is fitted to data with the least squares method. The massflow model has better fit for low load, i.e when the pressure ratio and massflow are low. The efficiency model seems to have better fit at higher pressure ratios. This is important to consider when designing the model to get a model that works well in a desired operating point. In the thesis a more general model is to be designed and the models are fitted to the engines whole operating range. More advanced compressormodels are presented in [19].

It is noticed that the high pressure compressor is more efficient at lower massflow than the low pressure compressor. This will be used in the controller, and is explained in chapter 6.

### 4.3.6 Validation turbine model

This section shows the validation of the turbine model described in section 4.2.4. The parametrization is made with least square curve fitting. The massflow model described in (4.23) gives a model that matches measured data as in figure below.

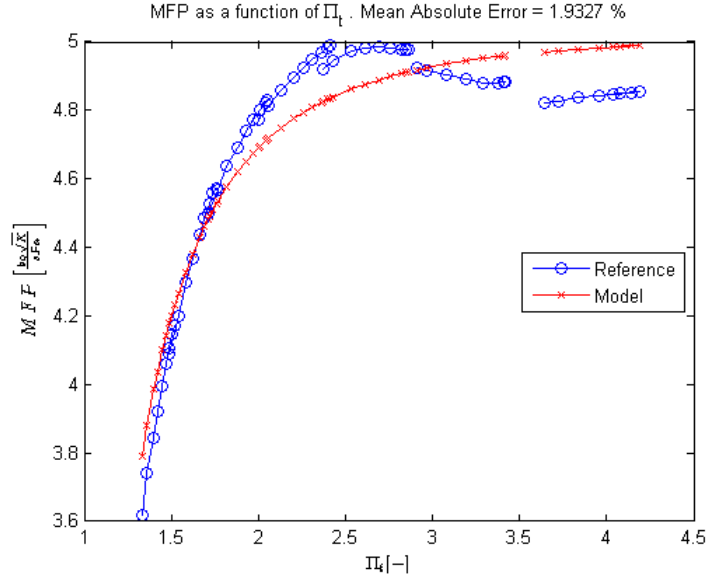
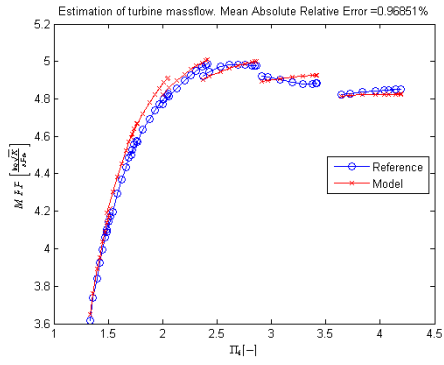


**Figure 4.8:** Validation of the massflow through the turbine. It is noticed that the model differ from the measured data for higher MFP and pressure ratio.

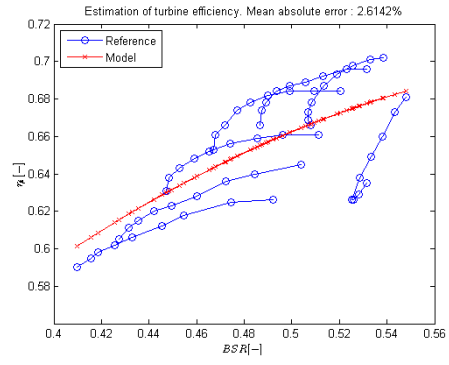
It is clear that the model does not capture a certain behaviour of the turbine, and by analyzing the model in section 4.2.4 it is noticed that the massflow is not a function of the turbine speed. Physically, higher turbine speed means higher massflow which is why a turbine speed dependency is added to the turbines massflow parameter according to (4.30) below.

$$MFP = (a_1 n_{t,red}^{a_2}) \sqrt{1 - \frac{1}{\Pi_t^{a_3 n_{t,red}}}} \quad (4.30)$$

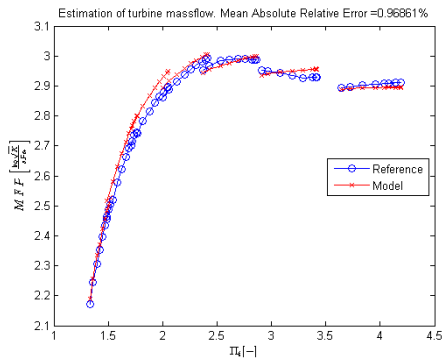
This gives a better results, which can be seen in figure 4.9 that shows the total validation of the two turboaggregates.



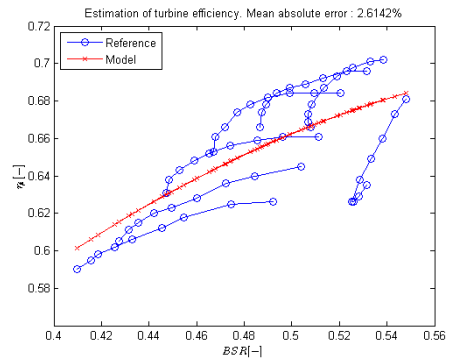
(a) Massflow validation, LPT



(b) Efficiency validation, LPT



(c) Massflow validation, HPT



(d) Efficiency validation, HPT

**Figure 4.9:** Validation of turbine model. First row is describing the low pressure turbine and the second row is describing the high pressure turbine.

Both models seems to match the measured data well in the whole operating range. The massflow model captures the turbine speed dependency well.

# Chapter 5

## Temperature model

This chapter describes how the existing exhaust gas temperature model may be improved.

### 5.1 Derivation of dynamic equations

The main goal is to add dynamics to the model to better be able to describe temperature transients. The chosen way of doing this is to add some thermodynamic inertia, namely the mass of the exhaust manifold. The mass will function as a lowpass filter since heat will transfer between the gases and the wall. In transients the temperature of the mass will not only vary with time, but also the distance from the heat source. See figure 5.1 below.

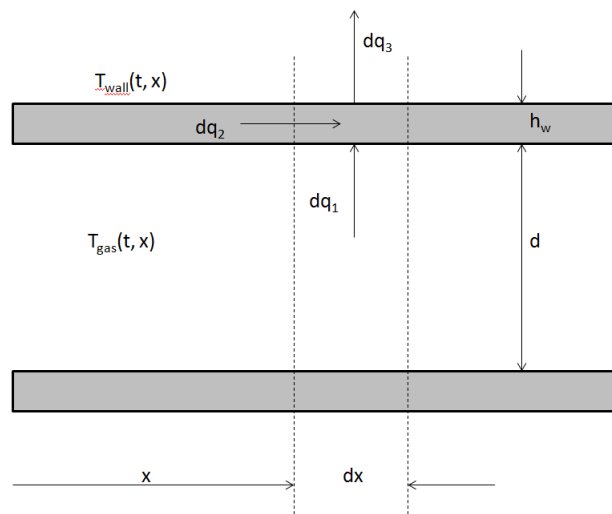


**Figure 5.1:** A descriptive figure of the exhaust manifold, which is divided into  $n$  pipe sections  $dx$ . General equations are stated for one section.

### 5.1.1 Gas temperature

Assume a pipe section  $dx$ . During the time  $dt$  a certain amount of mass and enthalpy will enter the section. The mass and enthalpy that leaves the pipe section will not only be a function of  $t$ , but also  $x$  since the density is not considered constant and the gas temperature vary with the varying wall temperature. This means that the inner energy is a function of both  $t$  and  $x$ . This is studied further in [22], and a governing dynamic equation is stated based on mass- and energyconservation. This equation is shown below.

$$\rho(x, t) \frac{\pi D^2}{4} \frac{\partial u}{\partial t} + (h(x, t) + u(x, t)) \frac{\partial \dot{m}_{gas}}{\partial x} = -\alpha \pi D (T_{gas}(x, t) - T_{wall}(x, t)) - \dot{m}_{gas} \frac{\partial h}{\partial x} \quad (5.1)$$

Where  $\rho$  is the gas density,  $D$  is the pipe diameter,  $h$  is the enthalpy,  $u$  is the entropy (inner energy) and  $\alpha$  is the heat transfer coefficient.

The equation above is derived from fundamental laws and is a general equation, valid for any type of fluid and flow characteristics. Since the fluid in this case is exhaust gas, an assumption that the fluid is an ideal gas seems reasonable. For ideal gases holds following.

$$h - u = pv = RT \quad (5.2a)$$

$$\frac{\partial u}{\partial t} = c_v \frac{\partial T}{\partial t} \quad (5.2b)$$

$$\frac{\partial h}{\partial t} = c_p \frac{\partial T}{\partial t} \quad (5.2c)$$

To achieve a fairly simple and computationally reasonable model, an assumption that the massflow does not change with the distance  $x$ .

$$\frac{\partial \dot{m}}{\partial x} = 0 \iff \frac{\partial \rho}{\partial t} = 0 \quad (5.3)$$

When taking a closer look at this assumption the conclusion might be that it is not to recommend. That is since the massflow in the exhaust port from the cylinder is strongly pulsating. The pulsations are spread into the exhaust manifold, which means that the massflow really does vary with the distance  $x$ . Nonetheless this assumption is made and motivated by the decreasing computational complexity and that the model is a mean value model that neglects the pulsations.

With these assumptions following model is obtained for the gas temperature.

$$\rho c_v \frac{\pi D^2}{4} \frac{\partial T_{gas}}{\partial t} = -\alpha \pi D (T_{gas} - T_{wall}) - \dot{m} c_p \frac{\partial T_{gas}}{\partial x} \quad (5.4)$$

According to [22] the time derivative of the exhaust manifold inlet temperature often is relatively small and can be neglected. The now even more simplified model can be expressed as follows.

$$\dot{m} c_p \frac{\partial T_{gas}}{\partial x} = -\alpha \pi D (T_{gas} - T_{wall}) \quad (5.5)$$

One important note is that the gas temperature in (5.5) is a function of both the distance  $x$  and the time  $t$ . That is since the wall temperature  $T_{wall}$  is a function of both  $x$  and  $t$ , and the massflow  $\dot{m}$  is a function of time. This final model is simplified in order to facilitate the implementation. When implemented and the analyzing of the model begins, it is important to have knowledge about these assumptions.

### 5.1.2 Wall temperature

Heat that is transferred from the gases to the pipe section  $dx$  during the time  $dt$  is described by (5.6) below, and is represented by  $dq_1$  in figure 5.1.

$$dq_1 = \alpha\pi D(T_{gas} - T_{wall}) dxdt \quad (5.6)$$

Heat losses to the surroundings from the pipe section  $dx$  during the time  $dt$  is made out of convection and radiation, who together are represented by  $dq_3$  in figure 5.1. This heat loss is expressed mathematically below, where the first term is representing convection, and the second term radiation.

$$dq_2 = \beta\pi D(T_{gas} - T_{wall})dxdt + \epsilon\sigma\pi(D + 2h_{wall})(W_{wall}^4 - T_a^4)dxdt \quad (5.7)$$

Conduction in the wall in the pipe section  $dx$  during the time  $dt$  is represented by  $dq_2$  in figure 5.1. The equation is shown below.

$$dq_3 = \lambda_{wall}\pi(h_{wall}^2 + Dh_{wall})\frac{\partial^2 T_{wall}}{\partial x^2} dxdt \quad (5.8)$$

The change in inner energy of the pipe sections mass is described as follows

$$\Delta u = \pi\rho_{wall}(h_{wall}^2 + Dh_{wall})c_{wall}\frac{\partial T_{wall}}{\partial t} dxdt \quad (5.9)$$

As for the gas temperature the law of energy conservation can be applied, which means that  $\Delta u = dq_1 + dq_3 - dq_2$ . This gives the following expression, which is the final model.

$$\begin{aligned} \rho_{wall}(h_{wall}^2 + Dh_{wall})c_{wall}\frac{\partial T_{wall}}{\partial t} dxdt = & (\alpha D(T_{gas} - T_{wall}) dxdt) + \\ & + \left( \lambda_{wall}(h_{wall}^2 + Dh_{wall})\frac{\partial^2 T_{wall}}{\partial x^2} dxdt \right) - \\ & - (\beta D(T_{gas} - T_{wall})dxdt + \epsilon\sigma(D + 2h_{wall})(W_{wall}^4 - T_a^4)dxdt) \end{aligned} \quad (5.10)$$

### 5.1.3 State space model

The temperature model can be represented in state space form by combining (5.5) and (5.10). To avoid computational complexity the convection in equation 5.10 is assumed to be dominant, and the other losses are neglected [10].

By dividing the exhaust manifold into  $n$  sections the derived equations may be rewritten as follows for section  $k$ .

$$\frac{dT_{wall,k}}{dt} = -\frac{\alpha D}{\rho_{wall}(h_{wall}^2 + Dh_{wall})c_{wall}}T_{wall,k} + \frac{\alpha D}{\rho_{wall}(h_{wall}^2 + Dh_{wall})c_{wall}}T_{gas,k} \quad (5.11a)$$

$$T_{gas,k} = \frac{\alpha\pi D}{\alpha\pi D - \dot{m}c_p}T_{wall,k} + \frac{-\alpha\pi D}{\alpha\pi D - \dot{m}c_p}T_{gas,k-1} \quad (5.11b)$$

Note that the model above may be expanded to also model the conduction and radiation according to equation 5.10. The input to the state space model is the gas temperature at the inlet,  $T_{gas,k-1}$ . The state is the wall temperature in the pipe section,  $T_{wall,k}$ , and the output is the gas temperature in the pipe section  $T_{gas,k}$ . If the inlet and outlet temperature together with the massflow is measured, it is possible to estimate the heat transfer coefficient. This is preferably done with a grey-box estimation in Matlabs System identification toolbox.

## 5.2 Temperature measurements

In the test cell there are two temperatures that are of special interest for the thesis, the cylinder out temperature and the turbine inlet temperature.

### 5.2.1 Experimental setup

The two temperatures are measured in different ways. The cylinder out temperature is measured directly after each exhaust port, i.e each cylinder has its own temperature sensor. The sensors are bored through the pipe flange connected to the engine block. Since the model is to describe a mean value engine, the mean value of all exhaust ports serve as cylinder out temperature.

Each cylinder has its own exhaust pipe. The pipes from cylinder one to three are connected, and the same goes for cylinder four to six. These two pipes leads the flow into the turbine, and the mean value of the temperature measured in each of these pipe connections describes the turbine inlet temperature. The two sensors are bored through a flange where the pipes are connected to the turbine. See figure 5.2 below.

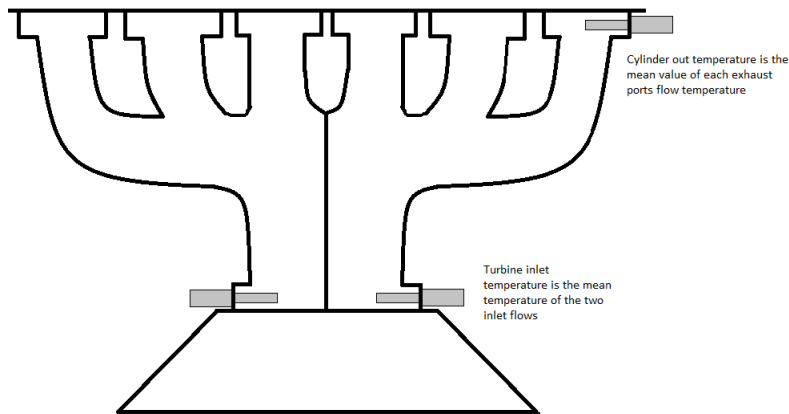


**Figure 5.2:** *An overview of the sensor placement in the exhaust manifold.*

In the dynamic experiments the engine is programmed to follow a response curve that makes steps in engine load at certain engine speeds. The stationary measurements are made out of several operating points where the engine is allowed to stabilize during a certain time.

## 5.2.2 Experimental results

Since no energy is added in the exhaust manifold and the heat flows described earlier indicates on losses to the engines environment via the manifold wall, the temperature would without doubt decrease towards the turbine. Clearly, after this experiment that is not the case. In figure 5.3 below, the above mentioned temperatures are plotted versus time during the transients, and the turbine inlet temperature is higher than the cylinder outlet temperature. According to theory this is surprising, and it leads to the question what actually is measured.

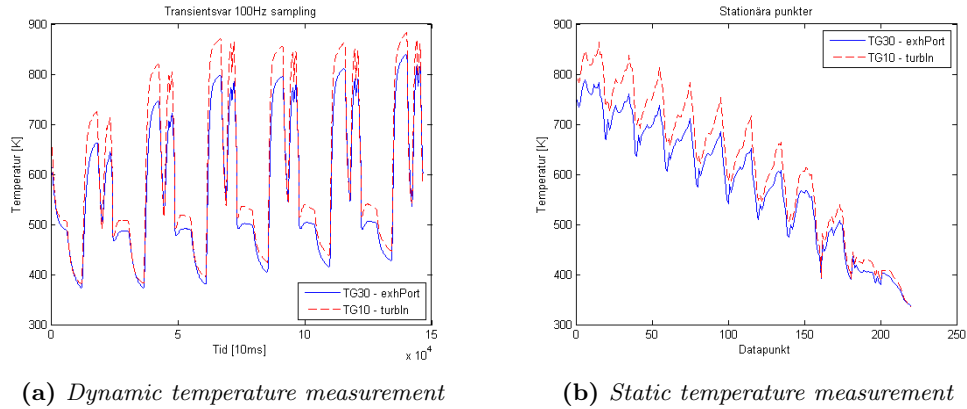


**Figure 5.3:** Exhaust manifold temperature measurement results. As seen above, the turbine inlet temperature is higher than the cylinder outlet temperature.

## 5.2.3 Temperature measurements

By comparing theory with the experimental results one can either trust theory or the measurements. In the thesis a lot of work has been made with the theoretical model and the level of trust for it is high. Therefore the temperature measurements are investigated. Figure 5.4 below shows an overview of the measurements made in the manifold.

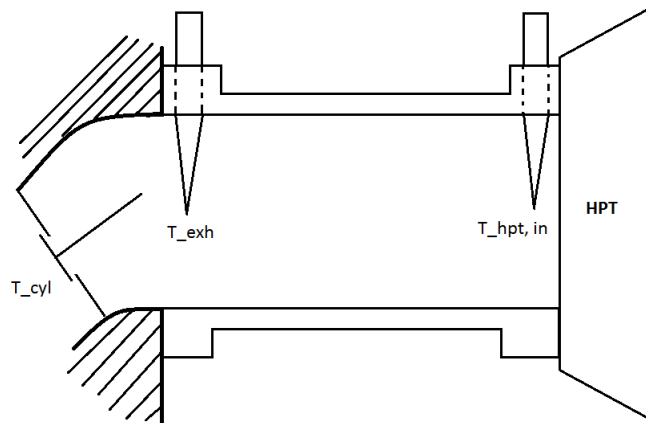


**Figure 5.4:** An overview of the temperature measurements made in the exhaust manifold.

The sensors are of thermocouple type. The principle of a thermocouple is that when two threads of different material are welded together and their temperature change, an electric

potential is introduced. This potential can be measured and related to a reference and the change in temperature.

There are a lot of different types of thermocouples with two variants especially interesting for the upcoming theory; isolated and exposed measurement. The isolated measurement has the welded connection of the threads safely placed inside a protection housing, and in the exposed measurement the connection is not protected. Logically, this means that the isolated measurement withstand higher temperatures. Because of this, the thermocouple used in the experiment is of isolated type, and has a diameter of 4 mm. See figure 5.5 for a closer look.

When the engine is operating it is cooled. In the dynamic experiment described above, the coolants temperature is about 363 K. The gas temperature may in the transients be as high as 870 K, see figure 5.3. When the temperature probe is inserted into the exhaust pipe the temperature gradient between the gas and the surroundings will introduce a heat flow in the protection housing. When the immersion depth decreases the temperature gradient will increase and therefore also the heat flow to the surroundings. This means that for decreasing immersion depth the measurement error will increase.

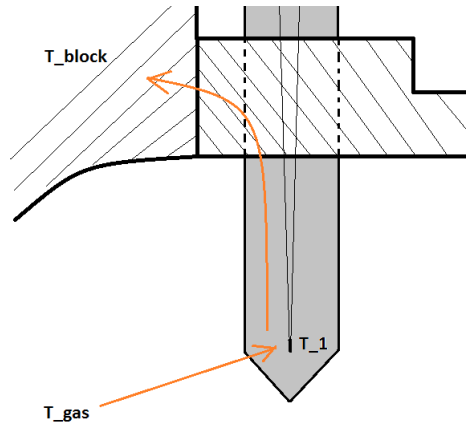
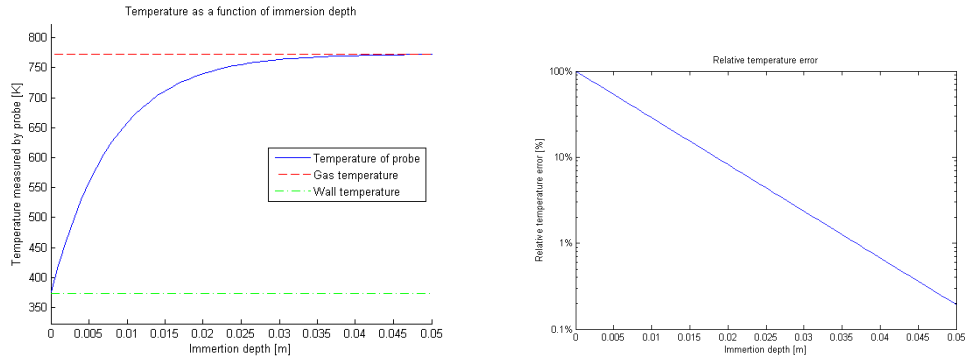


**Figure 5.5:** A closer look at the temperature sensor.

A model for the actual measured temperature as a function of immersion depth is suggested in [23], and can be rewritten as follows.

$$T_{meas} = (T_{wall} - T_{gas}) e^{\frac{-L}{D_{eff}}} \quad (5.12)$$

$T_{meas}$  is the measured temperature,  $T_{wall}$  is the wall temperature and  $T_{gas}$  is the gas temperature.  $L$  is the immersion depth and  $D_{eff}$  is the effective diameter of the probe. For the probes at the exhaust port the wall temperature is assumed to be close to the coolant temperature, ie 370 K. The gas temperature is considered to be 773 K. With this model and assumptions, the temperature measurement of the probe as a function of immersion depth is shown in figure 5.6. It is clear that the immersion depth influence the temperature measurement. For example, the common rule of thumb that the immersion depth shall be ten times the probe diameter can be motivated since the relative error for a depth of 40 mm is lower than 1 %.



(a) Measured temperature as a function of immersion depth (b) Relative error of the measurement as a function of immersion depth.

**Figure 5.6:** Illustration of the influence of immersion depth of the temperature probe.

According to in-house definitions, the sensors are inserted 3-4 mm inside the pipe center, with at least 40 mm insertion depth. This minimum depth is questionable since the diameter of the exhaust pipe is about 43 mm. If the tip of the probe is inserted 3 mm inside the center of a pipe with that diameter the immersion depth will be 20 mm. In this case, according to figure 5.6, the temperature is measured about 40 K wrong.

For a probe closer to the turbine the wall temperature will be higher. This is because energy is absorbed by the turbine and transferred to the compressor, and this process has an efficiency. The losses will create heat flow which is absorbed by the thermodynamic inertia made out of the turbine housing. If the wall temperature is higher, the temperature gradient will be lower, and therefore also the heat flow. The measured temperature error will be smaller. An illustration of this is shown in figure 5.7 below, where the measured temperature is described as a function of wall temperature. The immersion depth is fixed to 20 mm.

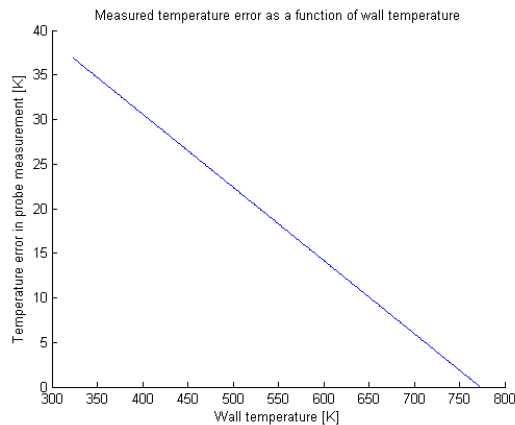


**Figure 5.7:** Measured temperature as a function of wall temperature. The immersion depth is 20 mm.

For example, if the wall temperature close to the turbine is 673 K, the measurement error is about 9 K. This means that the influence of the immersion depth is depending on the wall temperature, or more specifically the temperature gradient. A small temperature gradient means less heat flow and therefore smaller measurement error.

## 5.2.4 Suggested solution

A good start to analyze this problem would be to control how the probes are installed. The in-house regulations are contradictory since the minimum immersion depth is 40 mm but the pipe itself has a diameter of around 43 mm. Knowledge about how this is solved is sufficient for future work.

More advanced temperature measurements has been made at the cold side of the engine by the royal institute of technology [24]. Since the environments are a lot nicer at the cold side of the engine than post injection, an extremely thin thermocouple could be used. This has advantages in both isolation and time response. The experiment setup also allowed measurements at different points in a thin slice of the pipe, which resulted in a gas temperature profile for the pipe disk.

A similar approach would be interesting to apply at the exhaust manifold. The thermocouple would have to be chosen to be able to handle the tougher environment. The exhaust gas contain particles that may harm the thermocouple threads. The environmental conditions such as temperature and flow can be used to calculate a minimum diameter of the thermocouple threads that can stand for example flow forces. This is left for future work.

The mentioned approach is illustrated in figure 5.8 below.

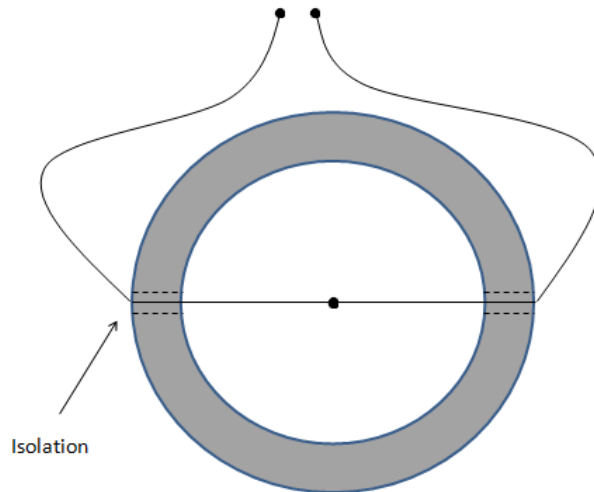


**Figure 5.8:** A suggested type of measurement. The thermocouple is implemented without protective housing, and the welded connection is placed where the temperature is to be measured. It is important to isolate the thermocouple connections to the manifold wall due to heat flow, as can be seen in section 5.2.3.



# Chapter 6

## Controller design

In this chapter the controller is shown and the process of designing it is explained. The main objective for the system control is to meet the demanded intake pressure since it is closely coupled to engine torque and thereby the driving experience.

### 6.1 Control problem

In diesel engines there are normally no throttle, the torque is only controlled by the amount of injected fuel. This is a more straightforward way of controlling the torque compared to a spark ignited engine. In a spark ignited engine lambda has to be more accurately controlled and therefore both air and fuel injections to the cylinder has to be controlled. However, the aftertreatment system of modern engines needs exhaust temperatures above a certain limit to operate optimally. To control the temperature, the flow through the system has to be controlled. This is often done by a throttle although the restriction has a cost in the form of a pressure loss.



**Figure 6.1:** The input and output of the engine control unit. The signal nomenclature is explained in appendix B.

To activate the turbochargers the exhaust gases is led through the turbines which drives the compressors. The energy in the gases is strongly coupled to the exhaust temperature - hot gases means more energy than cold. To control the compression of air on the inlet side, the speed of the compressor has to be controlled. Thereby the amount of air

flowing through the turbines have to be controlled, which is done with a bypass-valve called wastegate. In addition to this, it is important to have the right knowledge about the temperature of the gases, to be able to control how much energy that is put into the turbines.

The smaller turbocharger closest to the engine is also able to bypass the compressor on the inlet side. This is since it is a smaller charger, its speed might overshoot at high flows. To avoid dangerous operating points it is necessary to be able to deactivate this turbocharger fast. The bypass valve solves this problem.

The above mentioned actuators is used to control the intake pressure given the engine speed, amount of injected fuel and demanded intake pressure. The control unit is showed in figure 6.1 above. The signal nomenclature is explained in appendix B.

## 6.2 Control approach

In this section the overall plan to solve the problem is discussed. There are many ways of solving this problem, see 2.2. Some solutions are very complicated and complex, but in the thesis one objective is to keep it simple but still receive good results. Therefore the approach will be straightforward and hopefully easy to follow. Overall, the engines operating points are divided in to four modes, listed below.

1. Mode 0 - No turbocharging
2. Mode 1 - Only high pressure turbo active
3. Mode 2 - Both turbochargers active
4. Mode 3 - Only low pressure turbo active

How these modes are chosen and how the control is designed for each mode is described in the following sections.

### 6.2.1 Operating modes

The modes above are the foundation in the upcoming controller, since they describe how the turbocharger shall behave depending on the engines operating point.

One of the modes clearly stand out, mode 0. In this mode the demanded intake pressure is equal to, or below the ambient pressure. No turbocharging is needed, and the intake pressure will be controlled by the throttle. Since the throttle has a pressure loss and it is controlling the amount of air injected to the engine, it has a vital function for the engine. Because of this the throttle control will be made not only with a feedback link, but also with a feedforward. The feedback will be made with a PI-controller with anti-windup.

The other three mode needs to be able to interact smoothly with bumpless transitions. A midrange controller is used for mode 2, where both turbochargers are running together. For the other two modes, where the turbochargers are running individually, a feedback PID-controller with anti-windup is used. Since the reference in this case is the charging pressure which is not vital for the engine, only a feedback link is used.

### 6.2.2 Mapping of modes

The overall goal is to make the gas exchange as good as possible. This means that the ability to compress air always should be as good as the operating point allows. A straight

forward approach is to analyze the efficiency of the compressors and make the controller to always choose the best, most efficient solution. The controller should be able to make this choice with knowledge of engine speed and the demanded intake pressure.

If the modeled efficiency of the two turbochargers are plotted, some differences will be noticed. The smaller turbocharger, the high pressure turbo, has a its highest efficiency at lower massflow compared to the low pressure turbo. The demanded intake pressure, or the demanded pressure ratio for each turbocharger, almost does not affect the efficiency at all. A midrange area is set where the two turbos have their most effective zones, which is corresponding to mode 2 where both turbochargers are activated. In a real life situation this could be exemplified as if the driver makes a large step in load. At first the massflow will be low - the efficiency of the high pressure turbo is higher than for the low pressure turbo - which is why the high pressure turbo is chosen. That is mode 1. The massflow increases when the step in the demanded intake pressure is made, and the controller enters the midrange zone. This is mode 2 where the two turbos are working together. When the massflow is high, the low pressure turbo has the highest efficiency, which is why the high pressure turbo is shut down. This is mode 3 where only the low pressure turbo is activated. This example shows that the high pressure turbo helps the low pressure turbo to gain speed, and increases the compression efficiency at low massflow. The modeled efficiency for both turbochargers according to (4.17) are plotted together with the midrange zone and shown in figure 6.2 below.

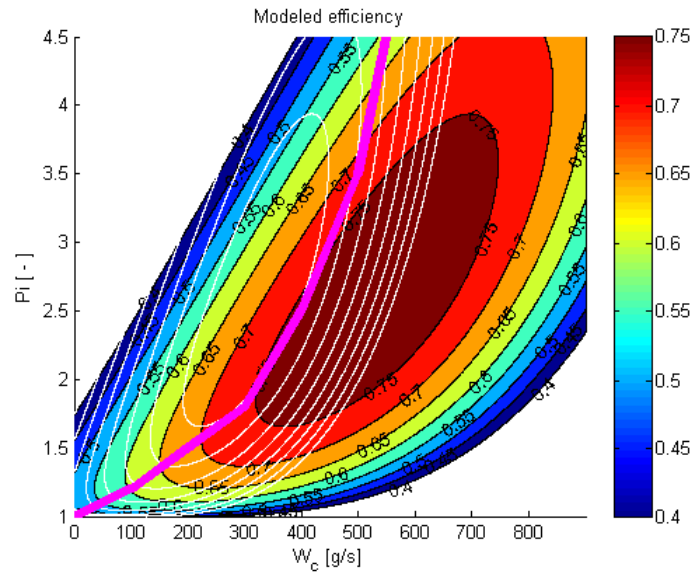


**Figure 6.2:** Modeled efficiency for the two turbochargers. The low pressure turbo is the filled-in contours, and the high pressure turbo is the white contours. The midrange zone is the magenta coloured curve.

With an assumption that the massflow through the compressors is equal to the massflow in to the cylinder (stationary conditions), (A.19) gives a way to express compressor massflow as a function of intake pressure and engine speed. This is plotted in figure 6.3 below. Some points from the midrange-curve are marked, and around them a midrange zone is created. This is the zone where the two turbochargers work together, coupled to engine speed and demanded intake pressure.

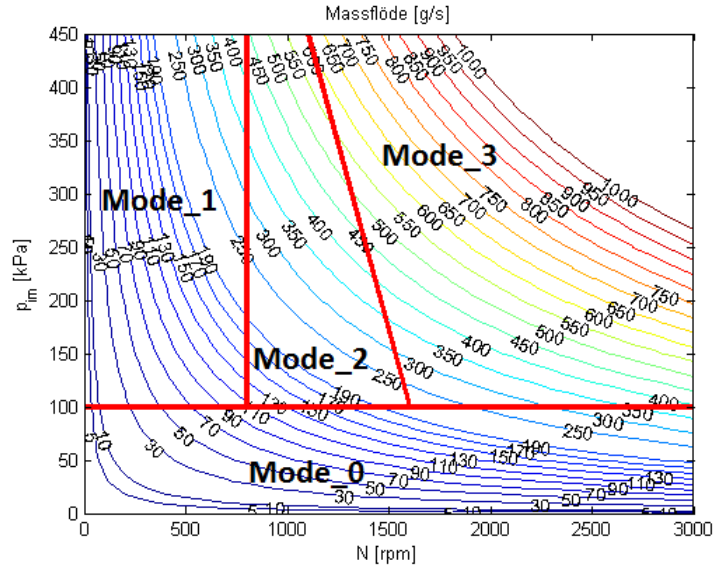


**Figure 6.3:** The defined modes. Mode 2 is corresponding to the midrange zone.

From these two plots the modes can be chosen with respect to compressor efficiency. What is happening in the different modes are explained in the following sections.

### 6.2.3 Mode 0

In this mode no turbocharging is needed, the demanded intake pressure is below ambient pressure. To reduce the pumping losses the wastegates should be opened, and only the throttle will control the intake pressure. The throttle controller is shown below.

#### Feedforward

By inverting (A.16), the control signal is expressed as a function of the throttle flowthrough area.

$$u(t)_{th,ff} = \frac{\arccos\left(1 - \frac{\left(\frac{A_{th,eff}(t)}{A_{th,max}}\right) - b_{th2}}{b_{th1}}\right) - a_{th2}}{a_{th1}} \quad (6.1)$$

Note that the trigonometric function above must be saturated to avoid computational problems. By assuming that the flow in to the cylinder is equal to the flow passing the throttle, (A.9) and (A.19) can be considered equal. Via the function below the effective flowthrough area can be calculated.

$$A_{th,eff} = f(p_{intake}, n_e, u_\delta, p_{exhaust}) \quad (6.2)$$

#### Feedback

The feedback link is made out of a PI-controller. Since the control signal contains a non-linearity in the form of a saturation the controller also handles the possible windup of the integral. The controller error is the difference between the actual intake pressure and its reference.

$$u(t)_{th} = K_P(p_{im,ref} - p_{im,act}) + I_{th,n} \quad (6.3)$$

$$I_{th,n} = I_{th,n-1} + K_P K_I T_s (p_{im,ref,n} - p_{im,act,n}) \quad (6.4)$$

The total control signal for the throttle is the sum of the feedback and feedforward links. The throttle is power by a servo, and the control signal is therefore limited, with lower limit  $u(t)_{min}$  and upper limit  $u(t)_{max}$ . The tracking part of the controller is a function of the difference between the saturated and non-saturated control signal. The equation is shown below.

$$I_{th,n} = I_{th,n} + K_I T_s (u(t)_{th,sat} - u(t)_{th}) \quad (6.5)$$

In above stated equation the tracking time-constant is chosen according to the rule of thumb  $T_{th,t} = T_{th,i}$ .

#### 6.2.4 Mode 1 and 3

In this mode one or the other turbocharger is activated individually. Since only one aggregate is active the reference will be the intake pressure. Since the throttle causes a pressure drop, this has to be added in the equations. This means that the real reference is the pressure after the intercooler. The controller works the same way for both aggregates, only the parameters differ. The feedback-link is made of a PID-controller with anti-windup. The equation for the controller is shown below.

$$u(t)_{wg} = K_P (p_{ic,ref} - p_{ic,act}) + K_I \int_0^t (p_{ic,ref} - p_{ic,act}) dt + K_D \frac{d}{dt} (p_{ic,ref} - p_{ic,act}) \quad (6.6)$$

The tracking part works the same way as for the throttle, with the exception that the tracking time-constant is chosen as  $T_{wg,i}$ . Obviously also the tuning parameters will differ to achieve satisfying results.

#### 6.2.5 Mode 2

In mode 2 the two turbochargers are activated at the same time. The high pressure turbo still has the intake pressure as reference. The reference to the low pressure turbo will in this mode be a calculated pressure corresponding to the other aggregates inlet pressure. This calculated reference will be a function of intake pressure and engine speed. Via the intake pressure two engine speeds can be calculated, and between these values a linear curve is tuned. This curve will describe the reference for the low pressure turbo. This is shown in figure 6.4 below.

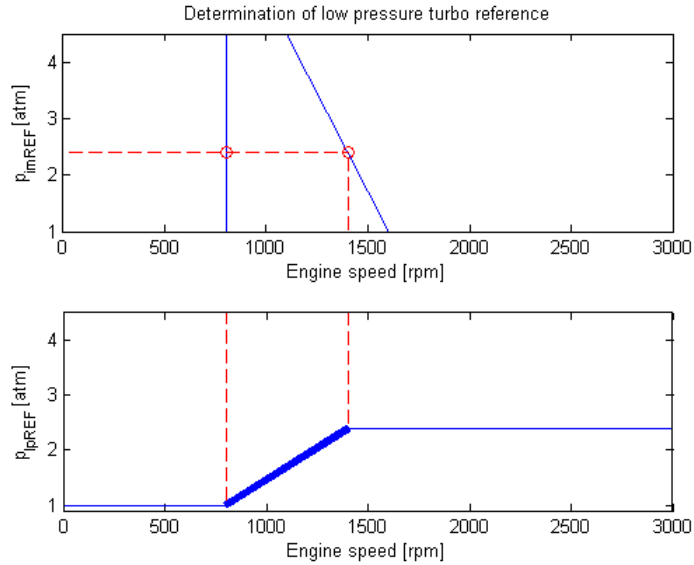


**Figure 6.4:** *Determination of pressure reference for low pressure turbo. The top curve describes how a certain intake manifold pressure correspond to a set of two engine speeds, between which the intake manifold pressure is to be translated to low pressure turbo reference. A linear slope is calculated between the two speeds, that is illustrated by the linear part of the lower plot. The pressure reference for the low pressure turbo is following this line. In this figure the intake pressure is 2.4 times the atmospheric pressure.*

Since the references are separated in this way the two aggregates can be controlled separately. The controllers are made out of PID-feedback links as for mode 1 and 3.

### 6.3 Safety application

When designing a turbocharger, certain material limitations has to be considered. In the thesis one of these limitations is studied - the speed limit. The speed is coupled to massflow, temperature and pressure which in certain high-load operating points may be dangerous for the turbo housing material. As a first approach the turbochargers speeds may be measured, which makes the problem quite straightforward since the speeds always are known. In the thesis another possibility is analyzed.

#### 6.3.1 Conditions and assumptions

The use of virtual sensors are often used to reduce production costs. In this case the problem is quite complex and to study how to make a high performing observer for both turbo speeds without adding sensors probably demands a lot of work. If even possible. The focus in the thesis is not to reduce the number of sensor, but to come up with an alternative to speed sensors. The goal is to have sufficient knowledge about the turbo speed at critical operating points to be able to reduce the control signal.

The massflow through the low pressure compressor is considered equal to the massflow through the throttle. This massflow is assumed always to be equal to the flow through the high pressure turbo. This is not always correct, but it seems to be a reasonable assumption. For example, when the bypass valve is opened, the flow through the high pressure compressors are lower than through the low pressure compressor. But since the

controller is designed in a way that the bypass valve only is opened when the high pressure wastegate is opened, there is no risk that the high pressure turbo cross the speed limit. Since the massflow is driven by pressure differences the pressure ratios of both compressors are considered known. Also, the upstream temperatures for each compressor is known. The conclusion is that the goal is to achieve a function as shown below.

$$\omega_c = f(\dot{m}_c, p_{us}, p_{ds}, T_{us}) \quad (6.7)$$

With the approach above the additional sensors will be temperature and pressure between the compressors.

### 6.3.2 Observer design

The equations 4.14, 4.15 and 4.16 in section 4.2.3 are inverted according to the following.

$$U_2^4 - \frac{K_2 \dot{m}_{thr}^2 T_{us}^2 16R^2}{p_{us}^2 \pi^2 D^4} U_2^2 = 4c_p^2 T_{us}^2 \left( \Pi_c^{\frac{\gamma-1}{\gamma}} - 1 \right)^2 K_1 \quad (6.8)$$

$$\omega_c = \frac{2U_2}{D} \quad (6.9)$$

The above stated equations gives four different solutions, where the right one has to be selected.

### 6.3.3 Limitation of control signal

Since the turbo speed can be observed the right actions have to be made by the controller. When the turbo is reaching a certain speed the control signal has to be limited. This is made according to the equation below.

$$u_{max} = \begin{cases} 1 - \frac{1}{k_\omega(\omega - \omega_{lim}) + 1} & \text{if } \omega \geq \omega_{lim} \\ 0 & \text{otherwise} \end{cases} \quad (6.10)$$

If the observed turbo speed is greater than the limit, the scaling  $k$  together with the speed difference will make the control signal to decrease. The turbo speed will therefore also decrease.



# Chapter 7

## Results

The performance of the designed system is evaluated and compared to single turbo engines, both with VGT and FGT. First a static point will be analyzed and compared between the models and also with measured data from an engine test cell. When the model is validated, transient tests will be evaluated.

### 7.1 Validation of model

A lot of effort has been put into the validation of the VGT model, see [1]. Since the turbo charging system differ from the two models, a comparison will be made without supercharging to validate that the engine match reality. This is done for a stationary operating point.

In figure 7.1 below, the serial turbo model is compared to the VGT model in a stationary operating point. It is clear that the models are not matching each other exactly. This is because the serial turbo has more complex models for control volumes and also an intercooler temperature model. In the comparison made below the two models are set to follow a certain intake pressure.

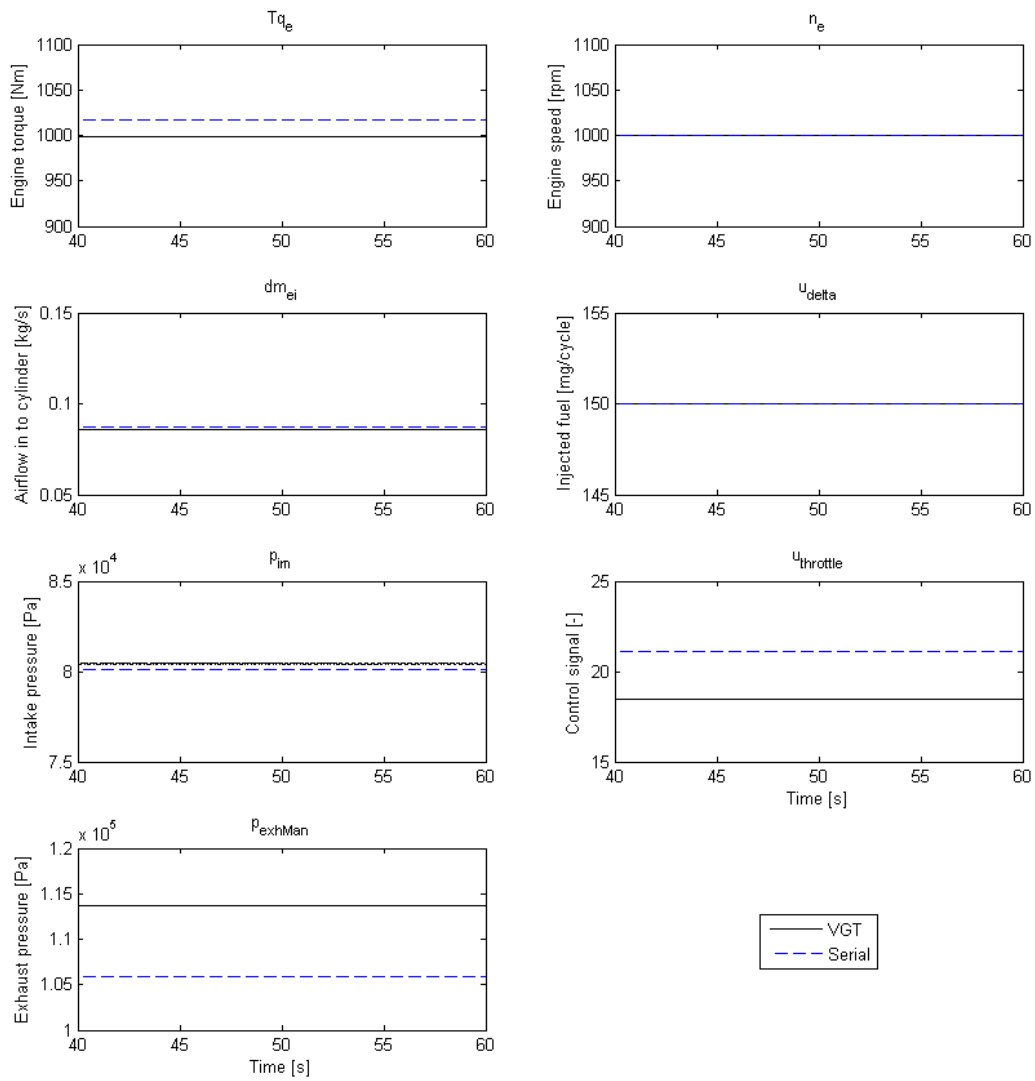


**Figure 7.1:** A comparison between the VGT model and the designed serial turbo. The engine is at constant speed 1000 rpm and the injected amount of fuel per cycle is 150 mg. Both turbochargers are disconnected. The values of the plotted signals match well. The small differences occur since the serial turbo has small differences in the model structure for control volumes and intake temperature.

## 7.2 Validation of controller

The controller is validated through two tests, one step response for intake pressure below ambient pressure to verify the throttle control and one step response for higher intake pressure to validate the wastegate controller. One should remember that the controllers have some tuning parameters that can be adjusted further if needed.

Normally the input to the engine is the pedal position set by the driver. This signal is interpreted to other signals for example engine speed and torque reference. In the thesis no driver interpreter is given, which is why this is handled manually by ramping the engine speed.

### 7.2.1 Throttle controller

The throttle controller is evaluated with a step made in intake pressure. The step is made below ambient pressure, when the engine is operating without turbocharging. See mode 0 in section 6.2.1. This type of evaluation for the serial turbo is made in figure 7.2 below.

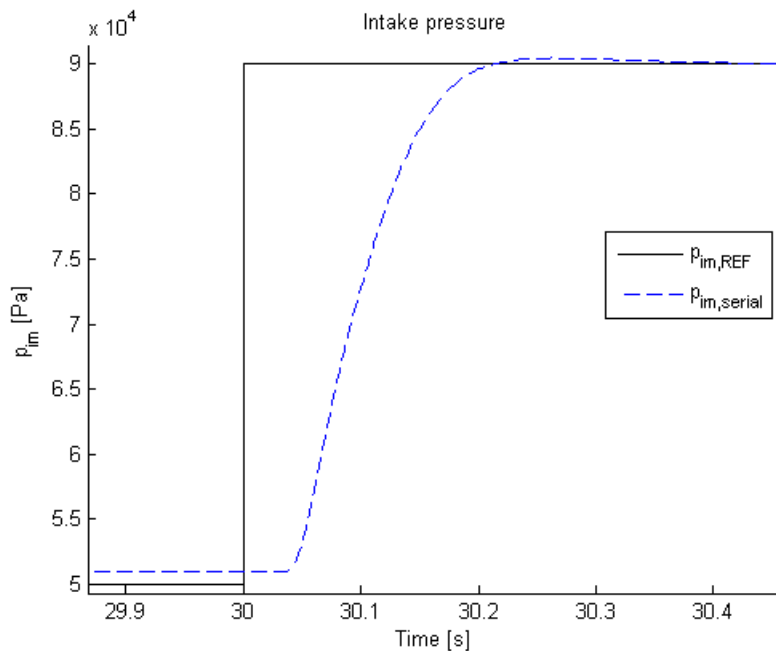


**Figure 7.2:** A step in intake pressure is made below ambient pressure to evaluate the throttle controller. The engine speed is set to 900 rpm and the amount of fuel is 150 mg/cycle. The solid line is the pressure reference and the dashed line is the actual intake pressure. The throttle dynamics including the delay is clearly shown. The controller follows the reference with good precision.

From this validation it is clear that the throttle controller works well and meets the requirements of following the reference.

### 7.2.2 Serial turbo controller

The controller described in section 6 is evaluated with a step in intake pressure and a ramp in in engine speed. The reason for ramping the engine speed is to execute all modes in the controller. The pressure step is set higher than ambient pressure since the controller is to control the wastegates that handle the aircharging.

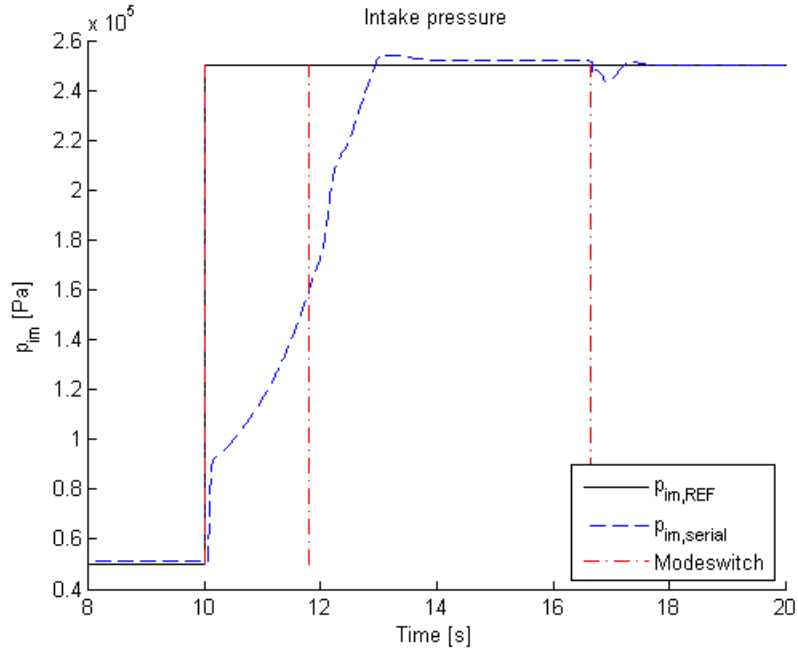


**Figure 7.3:** A step in intake pressure that executes all nodes. The pressure step is made from 0.5 bar to 2.5 bar, and the engine speed is ramped from 700 rpm to 1700 rpm with a slope of 500 rpm per second. The amount of injected fuel is 200 mg/cycle. That corresponds to the driver interpretation that executes all nodes. The pressure reference is followed nicely. When mode three is entered there is a small bump.

The controller follows the reference pressure well, except for a small bump when entering mode three.

Figure 7.3 does not describe how the turbochargers operate together and how the high pressure turbo is phased out. Figure 7.4 below shows the control signals and turbo speed of the turbochargers for the step described above. The controller handles the pressure step as planned. When controller enters mode one, the high speed turbine accelerates and starts to compress air. The wastegate by the low pressure turbo is still opened, and the small increase in speed is due to the increased massflow created by the high pressure turbo. When mode two enters the high pressure turbo starts to phase out and the low pressure turbo takes over. In mode three is the low pressure turbo the only activated turbocharger.

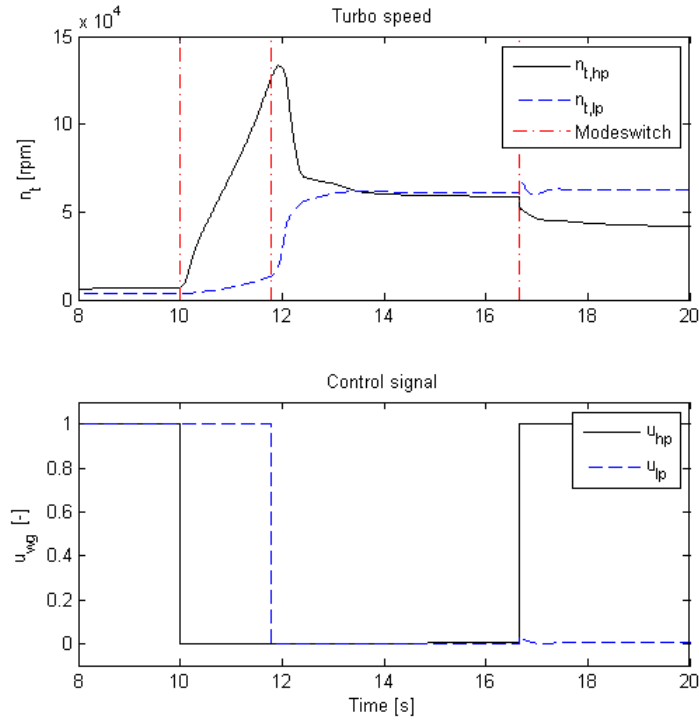


**Figure 7.4:** The lower plot is the signals controlling the wastegates, the other plot is the turbo speed. The vertical lines indicates where the different modes are entered. The engine input is the same as for figure 7.3.

### 7.2.3 Turbo speed observer

The observer is evaluated for the same engine input as for the validation of the two controller parts. The modeled turbo speed is plotted together with the observed speed in figure 7.5. The observer estimates the turbo speed well for higher speeds, which is the main objective since its purpose is to limit turbo speed when needed. It is noticed that the observer performance decreases after approximately 17 seconds. This is where the controller enters mode 3 and the bypass valve is opened, as described in section 6.3.1.

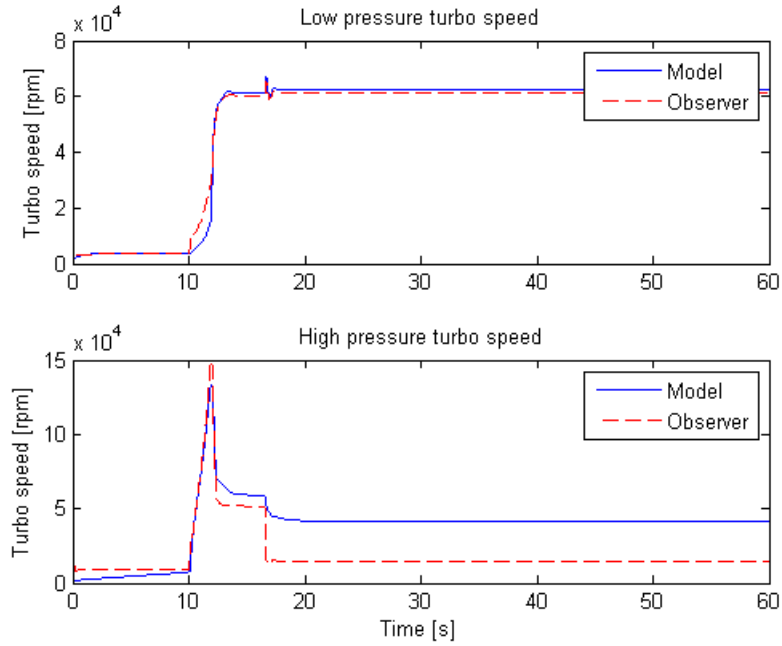


**Figure 7.5:** The observed turbo speed and the modeled turbo plotted against time. The engine speed is a ramp from 700 rpm to 1700 rpm with a slope of 500 rpm/s. The intake pressure step is set from 50kPa to 250kPa and the engine consumes 200 mg fuel per cycle.

It is clear that the observer is estimating the turbo speed with desired precision.

The observer is used to limit the turbo speed. In figure 7.6 the high pressure turbo speed is limited to 80000 rpm. It is clear that the safety application restricts the high pressure turbo to the desired limit.

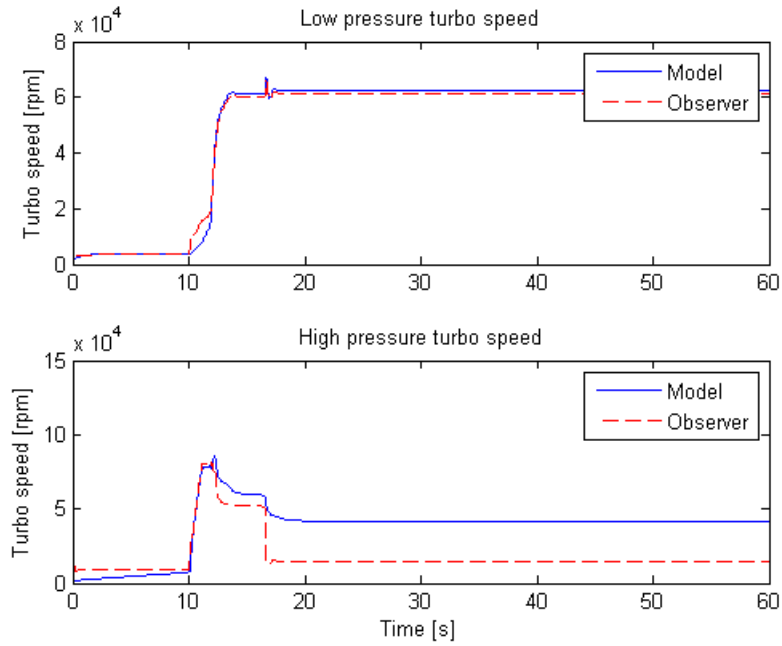


**Figure 7.6:** The safety application limits the high pressure turbo speed to 80000 revolutions per minute. The engine input is the same as in earlier case.

### 7.3 Simulation experiment

A simulation experiment is made to compare the VGT-charged engine with the serial sequential turbo charged engine.

A driving scenario is performed in both the VGT model and the serial turbo model. A step is made in intake pressure from 100 to 200 kPa and at the same time an engine speed ramp is initiated. The ramp starts at 600 rpm, has the slope 200 rpm per second and ends at 1600 rpm. The amount of injected fuel per cycle is 200 mg, and the oxygen to fuel ratio is limited to 1.2 (an approximate smoke limit). Figure 7.7 below, clearly shows a faster transient response for the serial turbo than for the VGT turbo. In the VGT-controller a simple, logic compensator has been implemented to lower the pumping losses. The added compensator opens the VGT bypass if the pressure difference over the cylinder becomes too high. To minimize the pumping losses caused by a too aggressive controller is a possibility to improve both systems. It is also noticed that the stationary massflow in to the cylinder is higher for the serial turbo.

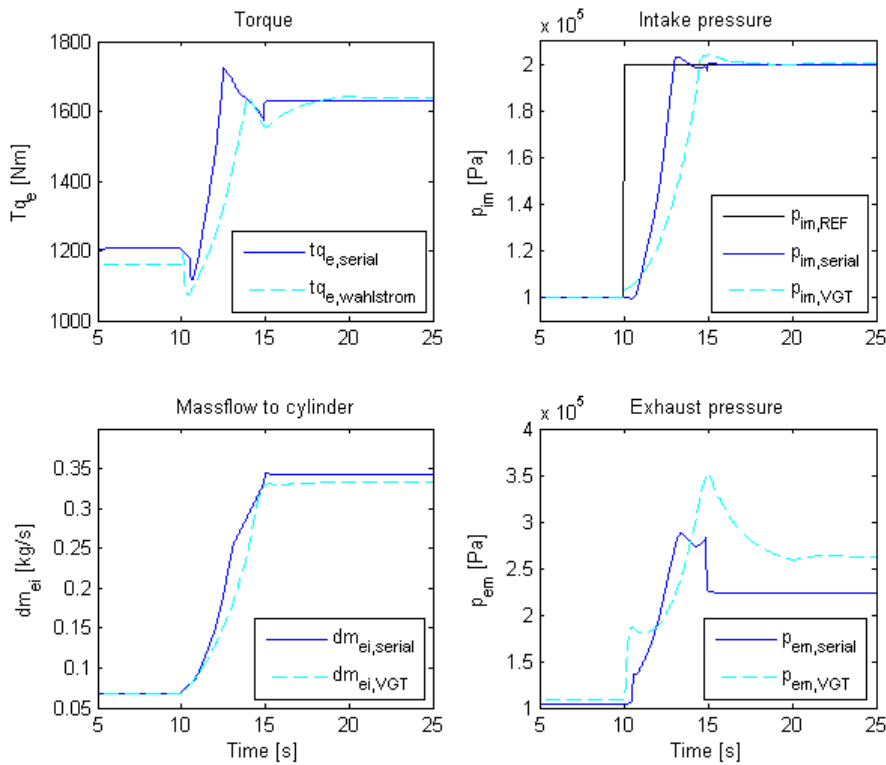


**Figure 7.7:** A comparison between the VGT-system and the serial turbo. The engine speed is ramped from 600 to 1600 rpm with a slope of 200 rpm per second, the intake pressure is a step from 100 to 200 kPa. The amount of injected fuel is 200 mg/cycle, and the oxygen to fuel ratio is limited to 1.2. It is clear that the serial turbo handles the transient faster than the VGT turbo due to the additional high pressure turbo. The controller is too simple to handle the pumping losses in a satisfying way. Also, the stationary massflow to combustion is higher for the serial turbo.

The higher massflow is a result of an increased volumetric efficiency. The volumetric efficiency is higher for the serial turbo since it has a lower pressure difference over the

cylinder. The volumetric efficiency is shown in figure 7.8 below. The oxygen to fuel ratio for the different charging systems are shown in the same figure. Note the limitation of  $\lambda_O$  at 1.2.

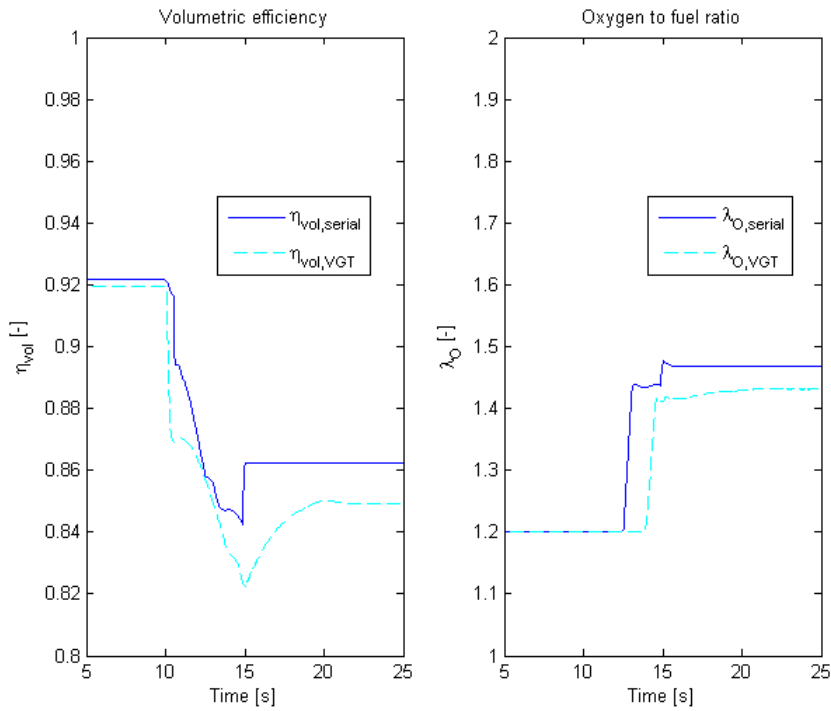


**Figure 7.8:** The volumetric efficiency is plotted as a function of time during the driving scenario described above. The serial turbo clearly has a better volumetric efficiency. The oxygen to fuel ratio is higher for the serial turbo system. Note the limitation at 1.2.

The turbo systems efficiencies is analyzed to conclude how well the turbochargers match the operating points in the driving cycle. Figure 7.9 below shows turbo speed, compressor efficiency and turbine efficiency for the two charging systems.

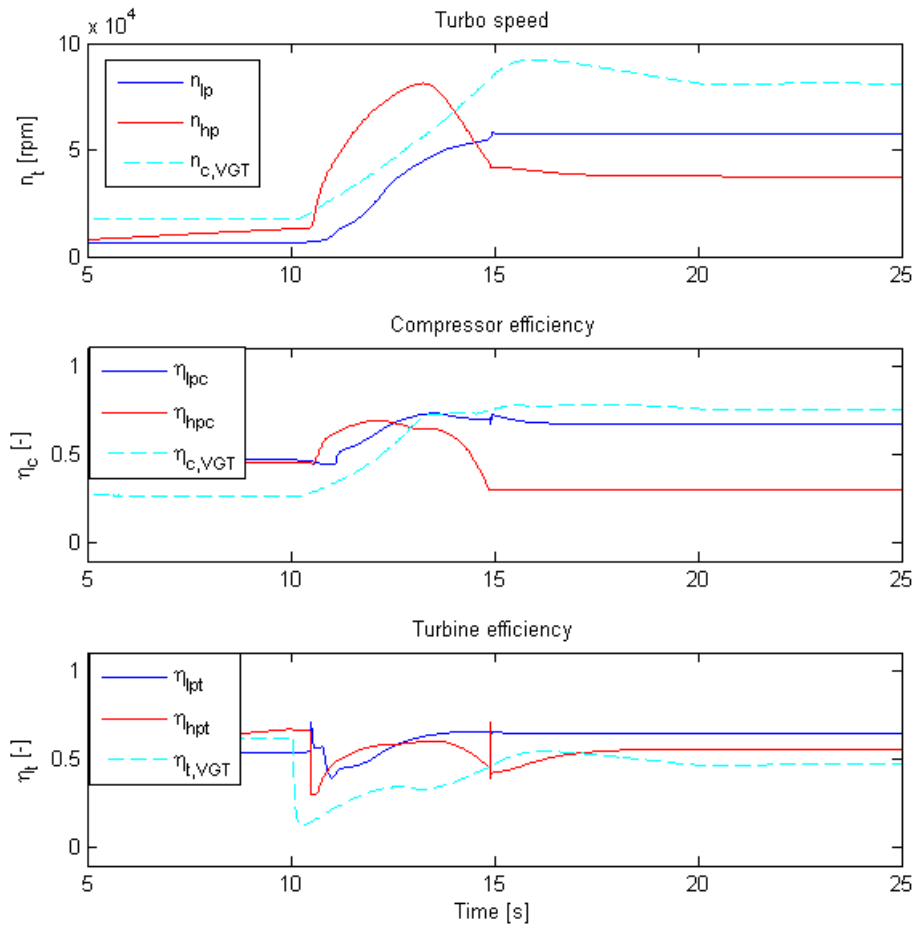


**Figure 7.9:** *Top:* The turbo speed during the driving scenario. The modeswitches for the serial turbo is highly visible. The stationary turbo speed is higher for the VGT compared to the low pressure turbo in the serial configuration. *Middle:* The compressor efficiency is higher for the VGT system compared to the serial turbo. Although the high pressure compressor efficiency is low at the stationary operating point, one should remember that the turbo is not used in that mode. *Bottom:* The turbine efficiency is overall better for the serial system compared to the VGT turbo.

The input values (engine speed and injected fuel per cycle) and the control signals that are set by the controller is shown in figure 7.10 below. The controller is a bit aggressive and builds up a high exhaust pressure. In future work this is recommended to take into account in the controller.

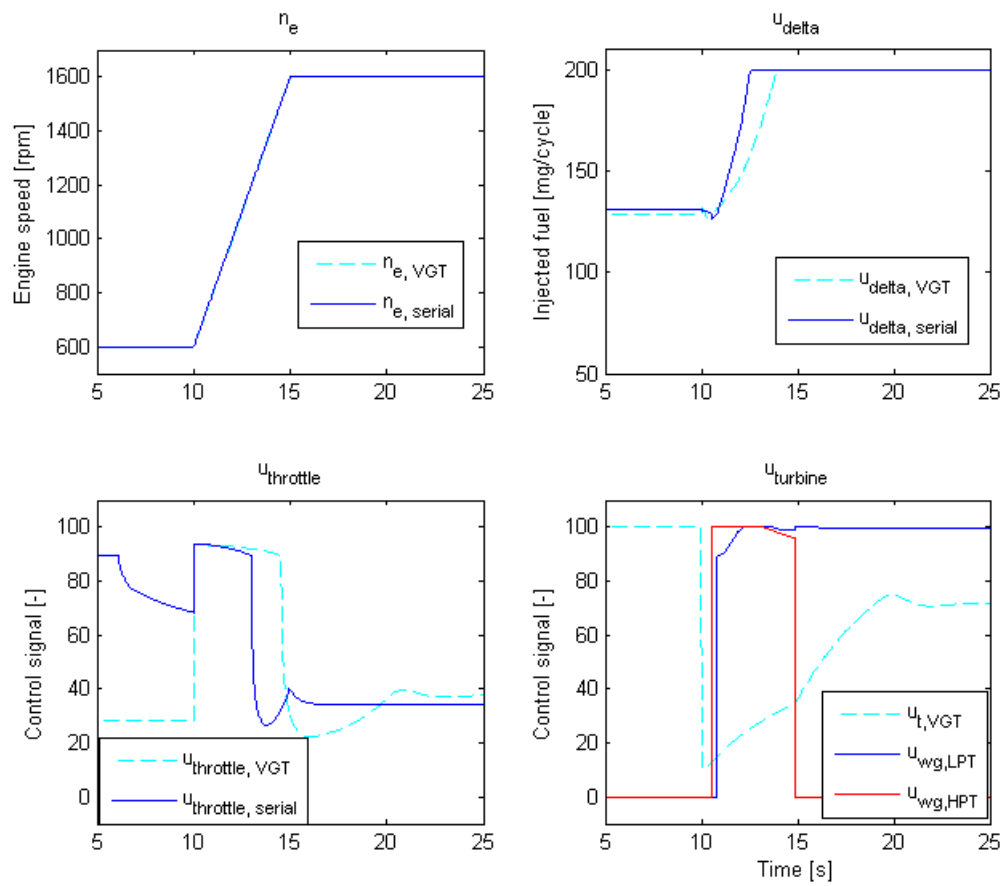


**Figure 7.10:** The engine speed and amount of injected fuel per cycle is set by a possible driver interpreter. The control signals to the turbo and the throttle are set by the controller.



# Chapter 8

## Conclusions and future work

A short summary of the thesis is given as well as suggestions of future work.

### 8.1 Conclusions

An engine model is developed and validated against the model created in [1]. The developed model has a different model structure for control volumes and intercooler, but the main difference is the supercharging system. The developed model has a serial turbo charging system with wastegated fixed geometry turbines.

A safe control system is designed to deliver the desired intake pressure without crossing the turbo chargers speed limits. This is done with PID-controllers with anti-windup, throttle control and a turbo speed observer. The control structure is quite simple and straightforward, based on modes dependant on the engine operating point.

The most obvious positive effect of the serial turbo system is the ability to increase the airflow fast and to higher levels compared to a single stage VGT turbo system. The increased airflow leads to the possibility to inject more fuel and achieve a higher torque. The conclusion will therefore be that the serial turbo is both able to deliver a demanded torque faster and also a higher stationary torque compared to the single stage system. This means that the serial turbo system may operate together with a smaller engine compared to the single stage VGT system, but they would still have the same performance. This is called downsizing.

One of the reasons to choose a VGT turbo is the increased efficiency in a wider operating range. Since the serial turbos high pressure stage increases the efficiency in a wider operating range naturally due to its lower inertia, a technically more robust solution such as a fixed geometry turbine with wastegate can be chosen.

The developed controller does not compensate the pumping losses occurring when wastegates are closing too aggressive. This would be something to consider as a possible improvement. The observer is quite simple but still observes the turbo speed with desired accuracy.

The trust in the model is high and is considered to make a good base for future work and add-ons. The controller seems to be too simple to really demonstrate the possible advantages in performance. However, some positive effects can be illustrated with only this simple control algorithm. The thesis gives a good hint of future possibilities, but for future implementation and maybe HIL-tests a lot of more testing and improvements in the controller has to be made.

## 8.2 Future work

A short collection of notes of possible improvements and add-ons are listed below. These are suggestions on future work.

### 8.2.1 Engine model

One long-term goal would be to end up with a model of a complete truck. That is why the connection to a driveline model such as the one in [6] is important. This connection needs more evaluation than made in the thesis.

The easiest way of connecting this engine model to a driveline model is probably to let the driveline demand a torque from the engine. To control that torque a fuel injector has to be modeled. When this is done, a driver interpreter would be interesting to develop so that the only input to the model is a gas pedal position.

### 8.2.2 Controller

The controller developed in the thesis is a simple one that still gives the desired behaviour. As can be seen during a literature study of the actual subject, more complex strategies may be implemented. It would be interesting to compare this simple solution in the thesis to one of these.

One weakness in the solution in the thesis is that the exhaust pressure is not considered at all in the controller. In some operating points it is noticed that the wastegate valves are a bit aggressive and causes large pumping losses. A start to a better solution would be to compensate for this in the controller, and analyze the improvement.

The simple observer limiting turbo speed that is implemented in this model may be improved. This is a complex and classic problem - how to estimate a state confidently without measuring it? The way to go is probably to analyze the minimum states that needs to be known and relate this to how they can be measured. For example, pressure is normally easier to measure than temperature. Is it possible to observe the turbo speeds without temperature measurements?

### 8.2.3 Temperature measurement

The temperature measurement method discussed in section 5.2.3 probably needs further examination. In the thesis only a brief analyze has been done. In section 5.2.4 a suggested solution or first step in the future examination is given. A lot of competence and knowledge exists, but needs to be concentrated to this problem. It would be interesting to see results from the suggested way of temperature measurement and compare them to the method used today. The suggested method will probably give results better matching the theory. Optimally, a test where also the wall temperature is measured should be performed. This may add knowledge about how much the engine block temperature and turbine housing temperature affects the gas temperature. The more knowledge about the system, the better the future model will be.

### 8.2.4 Temperature model

With better temperature data, the temperature model would be interesting to parameterize. One approach is to use a grey-box model with heat transfer coefficients for all three heat transfer forms as parameters. Once the model is validated, it would be interesting

to analyze how big influence the temperature dynamics has on the model and wastegate controller performance. Probably, the control will be improved since more knowledge about the temperature in transients is added. One interesting question is how big this improvement will be.

Next step would be to add more states in the model. The engine block temperature might be assumed constant since it is cooled, but the turbine housing temperature may vary a lot depending on turbine speed. Together with new and confirmed measurement methods this could result in a better model. However, the designer has to have the computational complexity in mind when adding states.



# Bibliography

- [1] J. Wahlström. *Control of EGR and VGT for Emission Control and Pumping Work Minimization in Diesel Engines*. PhD thesis, Linköpings Universitet, 2009.
- [2] K. Tufail T. Winstanley Y. Hardalupas AMKP. Taylor J. Black, PG. Eastwood. The effect of vgt vane control on pumping losses during full-load transient operation of a common-rail diesel engine. *SAE paper 2007-24-0063*, 2007.
- [3] FB. Basetti RF. Marsiglia. Thermodynamic evaluation of two-stage turbocharging system. *SAE paper 2012-36-0169*, 2012.
- [4] R.Stobart A. Plianos. Modeling and control of diesel engines equipped with a two-stage turbo-system. *SAE paper 2008-01-0118*, 2008.
- [5] S. Akehurst R. Burke G. Capon L. Smith S. Garret K. Zhang Z. Qingning, C. Brace. Simulation study of the series sequential turbocharging for enging downsizing and fuel efficiency. *SAE paper 2013-01-0935*, 2013.
- [6] J. Thornblad. Drivetrain modelling and clutch temperature estimation for heavy duty trucks. Master's thesis, Linköpings Universitet.
- [7] L. Eriksson. Modeling and control of turbocharged si and di engines. *Oil & Gas Science and Technology - Rev. IFP*, 62:523–538, 2007.
- [8] YY. Wang F.Chiara, M. Canova. An exhaust manifold pressure estimator for a two-stage turbocharged diesel engine. *Proc. Amer.Control Conf.*, pages 1549–1554, July 2011.
- [9] E. Mattarelli. Comparison among different 2-stage supercharging systems for hsd diesel engines. *SAE paper 2009-24-0072*, 2009.
- [10] L. Eriksson. Mean value models for exhaust system temperatures. *SAE paper 2002-01-0374*, 2002.
- [11] P. Moulin. Control of a two stage turbocharger on a diesel engine. *Joint 48th IEEE Conference on Decision and Control and 28th Chinese Control Conference*, pages 5200–5206, 2009.
- [12] J. Chauvin P. Moulin. Analysis and control of the air system of a turbocharged gasoline engine. *Proceedings of the 47th IEEE Conference on Decision and Control, Cancun, Mexico*, pages 5643–5649, December 2008.
- [13] J. Lunze A. Schanz D. Schwarzmann, R. Nitsche. Pressure control of a two-stage turbocharged diesel engine using a novel nonlinear imc approach. *IEEE International Conference on Control Applications, Munich, Germany*, pages 2399–2404, 2006.

- [14] P. Gautier A. Albrecht L. Fontvieiller A. Guinois L. Doléac A. Chasse, P. Moulin. Double stage turbocharger control strategies development. *SAE paper 2008-01-0988*, 2008.
- [15] S. Gunnarsson P. Lindskog L. Ljung J. Löfberg T. McKelvey A. Stenman J-E. Strömberg M. Enqvist, T. Glad. *Industriell Reglerteknik*. Reglerteknik, Institutionen för Systemteknik, Linköpings Universitet, 2010.
- [16] R. Stone M. Oldfield K. Kar, S. Roberts. Instantaneous exhaust temperature measurements using thermocouple compensation techniques. *SAE paper 2004-01-1418*, 2004.
- [17] L. Nielsen L. Eriksson. *Modeling and Control of Engines and Drivelines*. LiU-tryck, 2012.
- [18] O. Leufvén A. Thomasson L. Eriksson, T. Lindell. Scalable component-based modeling for optimizing engines with supercharging, e-boost and turbocompound concepts. *SAE paper 2012-01-0713*, 2012.
- [19] O. Leufvén. *Modeling for control of centrifugal compressors*. PhD thesis, Linköpings Universitet, 2009.
- [20] P. Andersson. *Air Charge Estimation in Turbocharged Spark Ignition Engines*. PhD thesis, Linköpings Universitet, 2005.
- [21] SAE standard. J922 - turbocharger nomenclature and terminology, 1988.
- [22] I. Shilling S. Richardson H. Fu, X. Chen. A one-dimensional model for heat transfer in engine exhaust systems. *SAE paper 2005-01-0696*, 2005.
- [23] JP. Tavener. Temperature calibration; depths of immersion. *Test and Measurement Conference*, 2006. [http://www.isotech.co.uk/files/document\\_library\\_file-10.pdf](http://www.isotech.co.uk/files/document_library_file-10.pdf).
- [24] F. Laurantzon. *Flow Measurements Related to Gas Exchange*. PhD thesis, Royal Institute of Technology, KTH, 2012.
- [25] A. Thomasson. *Modelling and control od actuators and co-surge in turbocharged engines*. PhD thesis, Linköpings Universitet, 2014.

# Appendix A

## Engine model

In this appendix the engine model equations are stated.

### Incompressible flow restriction

The enginemodel has three flow restriction that is modelled as incompressible (and adiabatic). In the model the massflow and temperatureflow through the component is calculated using the up- and downstream temperature and pressure. The airfilter, one part of the intercooler and the aftertreatment system is modelled this way.

#### *Input*

Variable	Unit	Description
$p_{us}$	Pa	Upstream pressure
$p_{ds}$	Pa	Downstream pressure
$T_{us}$	K	Upstream temperature
$T_{ds}$	K	Downstream temperature

#### **Output**

Variable	Unit	Description
$\dot{m}$	kg/s	Massflow through the component
$T$	K	Temperature of the massflow

#### *Parameters*

Variable	Unit	Description
$H_r$	$\text{Pa}^2\text{s}^2/\text{Kkg}^2$	Flow restriction coefficient
$p_{lin}$	Pa	Linearization pressure

#### *Equations*

$$\Delta p = p_{us} - p_{ds} \tag{A.1}$$

$$\dot{m} = \begin{cases} \sqrt{\frac{p_{us}\Delta p}{H_r T_{us}}} & \text{if } \Delta p \geq p_{lin} \\ \sqrt{\frac{p_{us}}{H_r T_{us}}} \frac{\Delta p}{\sqrt{p_{lin}}} & \text{otherwise} \end{cases} \quad (\text{A.2})$$

$$T = T_{us} \quad (\text{A.3})$$

By measuring  $\Delta p$  and  $T_{us}$  the parameter  $H_r$  can be estimated with the least square method. The parameter  $p_{lin}$  is used to avoid computational problem when  $\Delta p \rightarrow 0$  and is therefore set to a suitable value preventing this to happen.

## Control volume

In the enginemodel there are several control volumes that describes the volumes between all components, for example there is a volume between the airfilter and the low pressure compressor where the following model is used. The intake- and exhaust manifolds are modelled separate since they need to be able to describe additional physical processes. The control volumes has two states based on mass- and energyconservation.

### Input

Variable	Unit	Description
$\dot{m}_{us}$	kg/s	Massflow to the volume
$\dot{m}_{ds}$	kg/s	Massflow from the volume
$T_{ds}$	K	Downstream temperature
$T_{us}$	K	Upstream temperature
$\dot{Q}_{in}$	J/s	Heat transfer to the volume

### Output

Variable	Unit	Description
$p_R$	Pa	Pressure inside the volume
$T_R$	K	Temperature inside the volume

### Parameters

Variable	Unit	Description
$V$	$m^3$	Volume
$T_{init}$	K	Initial temperature
$p_{init}$	Pa	Initial pressure
$R$	J/kgK	Gas constant
$\gamma$	-	Heat capacity ratio

### Equations

$$\frac{d}{dt}\dot{m}_R(t) = \dot{m}_{us} - \dot{m}_{ds} \quad (\text{A.4})$$

$$\frac{d}{dt}\dot{T}_R(t) = \frac{1}{m_R} \left( \gamma\dot{m}_{us}T_{us} - \gamma\dot{m}_{ds}T_{ds} - (\dot{m}_{us} - \dot{m}_{ds})T_R + \frac{\dot{Q}_{us}}{c_v} \right) \quad (\text{A.5})$$

$$p_R = \frac{m_R R T_R}{V_R} \quad (\text{A.6})$$

An initial massflow  $\dot{m}_{init}$  is calculated according to the ideal gas law and the two parameters  $p_{init}$  and  $T_{init}$ . The volume  $V$  is known together with the gas property parameters  $\gamma$  and  $R$ .

## Intercooler

The purpose of having an intercooler is to cool the compressed air in order to increase the volumetric efficiency. This is done by leading the air through pipes that are cooled by a coolant. This coolant may be cooling water or turbulent air. The coolant is assumed to have a constant temperature  $T_{cool}$ . The model is built in two steps - step one describes how hard it is for the air to flow through the intercooler, step two describes how the temperature varies. Step one is described as an incompressible flow restriction according to 8.2.4. The temperature model is shown below, and is a simplified model that ignores the effects of the flow characteristics of the coolant.

### Input

Variable	Unit	Description
$\dot{m}_{ic}$	kg/s	Massflow through the intercooler
$T_{us}$	K	Upstream temperature
$p_{us}$	Pa	Upstream pressure
$p_{ds}$	Pa	Downstream pressure

### Output

Variable	Unit	Description
$T_{ic}$	Pa	Temperature from intercooler

### Parameters

Variable	Unit	Description
$a_1, a_2, a_3$	-	Constants in temperature function
$T_{cool}$	K	Temperature of the coolant

### Equations

$$T_{ic} = \max(T_{cool}, T_{us} + \epsilon(T_{us} - T_{cool})) \quad (\text{A.7})$$

$$\epsilon = a_1 + a_2 \frac{T_{us} - T_{cool}}{2} + a_3 \dot{m}_{ic} \quad (\text{A.8})$$

In the model above  $a_1$ ,  $a_2$  and  $a_3$  is estimated with the least square method by measuring all in- and outputs.

## Compressible flow restriction

In the throttle, bypass and the wastegates, the airflow may be so fast that its compression is affecting the massflow. That is why the massflow through these components is modelled as a compressible flow restriction. The input to the model is an effective flowthrough area, which is actuated by some kind of motor or pneumatic system. This model may cause problems when  $p_{us} = p_{ds}$  which means that the massflow derivative with respect to pressure ratio over the component reaches against negative infinity. To avoid such problems the model is linearized when close to these working points.

### Input

Variable	Unit	Description
$A_{eff}$	m <sup>2</sup>	Effectiv flowthrough are
$p_{us}$	Pa	Upstream pressure
$p_{ds}$	Pa	Downstream pressure

### Output

Variable	Unit	Description
$\dot{m}$	kg/s	Massflow through the component

### Parameters

Variable	Unit	Description
$\gamma$	-	Heat capacity ratio
$R$	J/kgK	Gas constant

### Equations

$$\dot{m}_{th} = \frac{p_{us} \Psi_{th}(\Pi_{th}) A_{eff}}{\sqrt{RT_{us}}} \quad (A.9)$$

$$\Psi_{th}(\Pi_{th}) = \begin{cases} \Psi_{th}^*(\Pi_{th}) & \text{if } \Pi_{th} \leq \Pi_{th,lin} \\ \Psi_{th}^*(\Pi_{th,lin}) \frac{1-\Pi_{th}}{1-\Pi_{th,lin}} & \text{if } \Pi_{th,lin} < \Pi_{th} \end{cases} \quad (A.10)$$

$$\Psi_{th}^*(\Pi_{th}) = \sqrt{\frac{2\gamma_{th}}{\gamma_{th}-1} \left[ \Pi_{th}^{\frac{2}{\gamma_{th}}} - \Pi_{th}^{\frac{\gamma_{th}+1}{\gamma_{th}}} \right]} \quad (A.11)$$

$$\Pi_{th} = \begin{cases} \left( \frac{2}{\gamma_{th}+1} \right)^{\frac{\gamma_{th}}{\gamma_{th}-1}} & \text{if } \frac{p_{im}}{p_{ic}} < \left( \frac{2}{\gamma_{th}+1} \right)^{\frac{\gamma_{th}}{\gamma_{th}-1}} \\ \frac{p_{im}}{p_{ic}} & \text{if } \left( \frac{2}{\gamma_{th}+1} \right)^{\frac{\gamma_{th}}{\gamma_{th}-1}} \leq \frac{p_{im}}{p_{ic}} \leq 1 \\ 1 & \text{if } 1 < \frac{p_{im}}{p_{ic}} \end{cases} \quad (A.12)$$

In the equations above the enthalpy is assumed to be constant, which means that the temperature is constant through the component.

## Throttle actuator

The throttle actuator dynamics is modelled as a first order system with a time delay. The effective flowthrough area is modelled as a trigonometric function. Actuator models is discussed further in [17], and in [25] more advanced models is described.

### Input

Variable	Unit	Description
$u_{th}$	-	Demanded signal, % of maximum flowthrough area

### Output

Variable	Unit	Description
$A_{th,eff}$	m <sup>2</sup>	Effective flowthrough area

### Parameters

Variable	Unit	Description
$\tau_{th}$	s	Timeconstant throttle
$\tau_{dth}$	s	Timedelay throttle
$a_{th1}, a_{th2}, b_{th1}, b_{th2}$	-	Parameters in trigonometric function

### Equations

$$w_{th} = \frac{1}{\tau_{th}} (u_{th}(t - \tau_{dth}) - \tilde{u}_{th}) \quad (\text{A.13})$$

$$\frac{d}{dt} \tilde{u}_{th} = \begin{cases} RL_{th} & \text{if } w_{th} > RL_{th} \\ w_{th} & \text{if } -RL_{th} \leq w_{th} \leq RL_{th} \\ -RL_{th} & \text{if } w_{th} < -RL_{th} \end{cases} \quad (\text{A.14})$$

The equations above is used to calculate the effective flowthrough area as shown below.

$$A_{th,eff} = A_{th,max} f_{th}(\tilde{u}_{th}) \quad (\text{A.15})$$

$$f_{th}(\tilde{u}_{th}) = b_{th1} (1 - \cos(\min(a_{th1}\tilde{u}_{th} + a_{th2}, \pi))) + b_{th2} \quad (\text{A.16})$$

By analyzing stepresponses in throttleposition, the timeconstant  $\tau_{th}$  and the timedelay  $\tau_{dth}$  can be determined. To calculate  $a_{th1}, a_{th2}, b_{th1}$  and  $b_{th2}$  stationary measurements are required to invert (A.9).

## Intake manifold

The intake manifold is modelled as a control volume according to 8.2.4, but with an addition that describes the oxygen concentration of the gas. This model is prepared to describe EGR.

### Input

Variable	Unit	Description
$\dot{m}_{us}$	kg/s	Upstream massflow
$\dot{m}_{ds}$	kg/s	Downstream massflow
$T_{thr}$	K	Temperature throttle
$T_{egr}$	K	Temperature EGR
$\dot{Q}_{in}$	J/s	Heat transfer to the volume
$X_{Oem}$	-	Oxygen concentration in the exhaust manifold

### Output

Variable	Unit	Description
$p_{im}$	Pa	Intake pressure
$X_{Oim}$	-	Oxygen concentration in the intake manifold

### Parameters

Variable	Unit	Description
$V_{im}$	m <sup>3</sup>	Volume
$T_{init}$	K	Initial temperature
$p_{init}$	Pa	Initial pressure
$R$	J/kgK	Gas constant
$X_{Oc}$	-	Oxygen concentration passing the compressor

### Equations

The volume itself is modelled as in 8.2.4, but in order to describe the oxygen concentration (and EGR when wanted) the equations below is added to the intake manifold model.

$$x_{egr} = \frac{W_{egr}}{W_c + W_{egr}} \quad (\text{A.17})$$

$$\frac{d}{dt} X_{Oim} = \frac{R_a T_{im}}{p_{im} V_{im}} ((X_{Oem} - X_{Oim}) W_{egr} + (X_{Oc} - X_{Oim}) W_c) \quad (\text{A.18})$$

## Cylinder

The cylinder model is quite big. It is divided into three parts - one for temperature, one for flow and one for torque. The following approach is based on the Seiliger cycle which describes the combustion in two stages - one part with constant volume and one part with constant pressure [1].

### Input

Variable	Unit	Description
$p_{us}$	Pa	Upstream pressure
$p_{ds}$	Pa	Downstream pressure
$X_{Oim}$	-	Oxygen concentration in the intake manifold
$n_e$	rpm	Engine speed
$u_\delta$	mg/cykel	Amount of injected fuel
$T_{im}$	K	Temperature in the intake manifold

### Output

Variable	Unit	Description
$\dot{m}_{ei}$	kg/s	Massflow in to the cylinder
$\dot{m}_{eo}$	kg/s	Massflow out from the cylinder
$T_{ds}$	K	Downstream temperature
$X_{Oe}$	-	Oxygen concentration in gas after combustion

### Parameters

Variable	Unit	Description
$V_d$	$m^3$	Displacement
$c_{vol1}, c_{vol2}, c_{vol3}$	-	Constants in volumetric efficiency model
$R$	J/kgK	Gas constant
$n_{cyl}$	-	Number of cylinders
$(A/F)_s$	-	Stoichiometric air/fuel ratio
$X_{Oc}$	-	Oxygen concentration passing the compressor
$q_{HV}$	J/kg	Energy density of the fuel
$x_{cv}$	-	The fraction of fuel burnt under constant volume
$c_v$	J/kgK	Specific heat capacity
$r_c$	-	Compression ratio
$\gamma$	-	Ratio of specific heat
$\eta_{sc}$	-	Compensation for non-ideal Seiliger cycle
$T_{amb}$	K	Ambient temperature
$h_{tot}$	$W/m^2K$	Heat transfer coefficient
$d_{pipe}$	m	The exhausts pipe diameter
$l_{pipe}$	m	The exhausts pipe length
$n_{pipe}$	-	Number of pipes in the exhaust
$\eta_{igch}$	-	Combustion efficiency
$c_{fric1}, c_{fric2}, c_{fric3}$	-	Constants in friction model

## Equations

### Flow model

$$\dot{m}_{ei} = \frac{\eta_{vol} p_{im} n_e V_d}{120 R_a T_{im}} \quad (\text{A.19})$$

$$\eta_{vol} = c_{vol1} \frac{r_c - \left(\frac{p_{em}}{p_{im}}\right)^{\frac{1}{\gamma_e}}}{r_c - 1} + c_{vol2} \dot{m}_f^2 + c_{vol3} \dot{m}_f + c_{vol4} \quad (\text{A.20})$$

$$\dot{m}_f = \frac{10^{-6}}{120} u_\delta n_e n_{cyl} \quad (\text{A.21})$$

$$\dot{m}_{eo} = \dot{m}_f + \dot{m}_{ei} \quad (\text{A.22})$$

$$\lambda_O = \frac{\dot{m}_{ei} X_{Oim}}{\dot{m}_f (O/F)_s} \quad (\text{A.23})$$

$$X_{Oe} = \frac{\dot{m}_{ei} X_{Oim} - \dot{m}_f (O/F)_s}{\dot{m}_{eo}} \quad (\text{A.24})$$

### Temperature model

$$T_e = T_{im} + \frac{q_{HV} f_{Te}(\dot{m}_f, n_e)}{c_{pe} \dot{m}_{eo}} \quad (\text{A.25})$$

$$f_{Te}(W_f, n_e) = f_{TeWf}(W_f) f_{Tene}(n_e) \min(\lambda_O, 1) \quad (\text{A.26})$$

$$f_{TeWf}(W_f) = c_{fTeWf1} W_{f,norm}^3 + c_{fTeWf2} W_{f,norm}^2 + c_{fTeWf3} W_{f,norm} + c_{fTeWf4} \quad (\text{A.27})$$

$$f_{Tene}(n_e) = c_{fTene1} n_{e,norm}^2 + c_{fTene1} n_{e,norm} + 1 \quad (\text{A.28})$$

$$W_{f,norm} = W_f \cdot 100 \quad (\text{A.29})$$

$$n_{e,norm} = \frac{n_e}{1000} \quad (\text{A.30})$$

$$T_{em,in} = T_{amb} + (T_e - T_{amb}) e^{-\frac{h_{tot} \pi d_{pipe} l_{pipe} n_{pipe}}{\dot{m} c_{pe}}} \quad (\text{A.31})$$

*Torque model*

$$M_e = M_{ig} - M_p - M_{fric} \quad (\text{A.32})$$

$$M_p = \frac{V_d}{4\pi} (p_{ds} - p_{us}) \quad (\text{A.33})$$

$$M_{ig} = \frac{u_\delta 10^{-6} n_{cyl} q_{HV} \eta_{ig}}{4\pi} \quad (\text{A.34})$$

$$\eta_{ig} = \eta_{igch} \left( 1 - \frac{1}{r_c^{\gamma-1}} \right) \quad (\text{A.35})$$

$$M_{fric} = \frac{V_d}{4\pi} 10^5 (c_{fric1} n_{eration}^2 + c_{fric2} n_{eration} + c_{fric3}) \quad (\text{A.36})$$

$$n_{eration} = \frac{n_e}{1000} \quad (\text{A.37})$$

The parameters in the flow model is estimated by fitting the curve describing  $\dot{m}_{ei}$ . This requires stationary measurements of  $x_{egr}$  and  $\dot{m}_c$  or  $\dot{m}_{ei}$  because  $\dot{m}_{ei} = \dot{m}_c / (1 - x_{egr})$ . The parameters of the temperature- and torque model is estimated in the same way but with other objective functions, for example  $(T_{em} - T_{em,meas})^2$  and  $(M_e + M_p - M_{e,meas} - M_{p,meas})^2$  respectively. This is depending on what measurements are available.

## Exhaust manifold

The exhaust manifold is modeled the same way as the intake manifold. The only differences are the in- and outputs and the values of the parameters.

### Input

Variable	Unit	Description
$\dot{m}_{eo}$	kg/s	Massflow from cylinder
$\dot{m}_{egr}$	kg/s	Massflow to EGR valve
$T_{em}$	K	Temperature in exhaust manifold
$\dot{Q}_{in}$	J/s	Heat transfer to the volume
$\dot{m}_t$	kg/s	Massflow to high pressure turbine
$X_{Oe}$	-	Oxygen concentration in the exhaust

### Output

Variable	Unit	Description
$p_{em}$	Pa	Pressure in the exhaust manifold
$X_{Oem}$	-	Oxygen concentration in the exhaust manifold

### Parameters

Variable	Unit	Description
$V$	m <sup>3</sup>	Volume
$p_{init}$	Pa	Initial pressure
$R_e$	J/kgK	Gas constant
$\gamma$	-	Ratio of specific heats

### Equations

$$\frac{d}{dt}p_{em} = \frac{R_e T_{em}}{V_{em}} (W_{eo} - W_t - W_{egr}) \quad (\text{A.38})$$

$$\frac{d}{dt}X_{Oem} = \frac{R_e T_{em}}{p_{em} V_{em}} ((X_{Oe} - X_{Oem})W_{eo}) \quad (\text{A.39})$$

The parameters in this model can be measured by hand if they are not given in a product specification.



# Appendix B

## Nomenclature

Table B.1 The variables used in the engine controller unit.

<b>Name</b>	<b>Description</b>	<b>Unit</b>
$u_\delta$	Injected amount of fuel	$mg/cycle$
$dm_{hpc}$	Massflow through the high pressure compressor	$kg/s$
$p_{hpc}$	Pressure after high pressure compressor	$Pa$
$t_{lpc}$	Temperature after low pressure compressor	$K$
$p_{airFilter}$	Pressure after air filter	$Pa$
$t_{airFilter}$	Temperature after air filter	$K$
$dm_{lpc}$	Massflow through the low pressure compressor	$kg/s$
$p_{lpcACT}$	Actual pressure after low pressure compressor	$Pa$
$p_{em}$	Pressure in exhaust manifold	$Pa$
$p_{im}$	Pressure in intake manifold	$Pa$
$p_{ic,ACT}$	Actual pressure in after intercooler	$Pa$
$n_e$	Engine speed	$rpm$
$p_{im,REF}$	Actual pressure in intake manifold	$Pa$

## Upphovsrätt

Detta dokument hålls tillgängligt på Internet – eller dess framtida ersättare – från publiceringsdatum under förutsättning att inga extraordinära omständigheter uppstår.

Tillgång till dokumentet innebär tillstånd för var och en att läsa, ladda ner, skriva ut enstaka kopior för enskilt bruk och att använda det oförändrat för icke-kommersiell forskning och för undervisning. Överföring av upphovsrätten vid en senare tidpunkt kan inte upphäva detta tillstånd. All annan användning av dokumentet kräver upphovsmannens medgivande. För att garantera äktheten, säkerheten och tillgängligheten finns lösningar av teknisk och administrativ art.

Upphovsmannens ideella rätt innefattar rätt att bli nämnd som upphovsman i den omfattning som god sed kräver vid användning av dokumentet på ovan beskrivna sätt samt skydd mot att dokumentet ändras eller presenteras i sådan form eller i sådant sammanhang som är kränkande för upphovsmannens litterära eller konstnärliga anseende eller egenart.

För ytterligare information om Linköping University Electronic Press se förlagets hemsida <http://www.ep.liu.se/>

## Copyright

The publishers will keep this document online on the Internet – or its possible replacement – from the date of publication barring exceptional circumstances.

The online availability of the document implies permanent permission for anyone to read, to download, or to print out single copies for his/hers own use and to use it unchanged for non-commercial research and educational purpose. Subsequent transfers of copyright cannot revoke this permission. All other uses of the document are conditional upon the consent of the copyright owner. The publisher has taken technical and administrative measures to assure authenticity, security and accessibility.

According to intellectual property law the author has the right to be mentioned when his/her work is accessed as described above and to be protected against infringement.

For additional information about the Linköping University Electronic Press and its procedures for publication and for assurance of document integrity, please refer to its www home page: <http://www.ep.liu.se/>.